

Chapter 9

Critical Evaluation of MA20 Abrasion Test

9.1 Introduction

In chapter eight a method of measuring and quantifying abrasion-wear in concrete pavers was developed. This included a system of classifying pavers in terms of various degrees of abrasion-wear, which will enable end users to specify a particular long term aesthetic look or degree of serviceability.

What is now required is an accelerated abrasion test to determine the 28-day abrasion resistance of factory made blocks prior to dispatch. If a relationship between this test and the wear on site can be established (the focus of chapter 14), then a means exists to predict the long-term performance of the blocks.

This chapter focuses on the first of three abrasion tests examined, the MA20 test, developed in Australia.

Considering the review of 32 abrasion tests done by the Australians, their research into the abrasion problem, and the eventual inclusion of this test as an interim abrasion test in their national specification, MA20(1986), it seemed logical to benefit from their results by including this test in this investigation. In this chapter the term 'MA20' will generally refer to this interim abrasion test.

9.2 Description of Test

This test is fully described and illustrated in 4.8. Briefly, the test involves abrasion of the paver surface by loaded ball bearings rapidly revolving over the surface. Water is used both to lubricate the race-way and to remove debris. An index, representing the abrasion resistance of the block under test, is derived from the penetration of the balls after 5000 revolutions. The resultant imprint of the test is a circular groove on the block, generally varying in depth from one to three millimetres.

9.3 Historical Background

The mechanism of abrasion of the MA20 test may be described generically as 'loaded revolving steel balls'. This places this test in a family of abrasion tests that are described in appendices U.2.09 through U.2.16, (see also table 4.1 of volume 2).

Tests of this kind were already operational in the USA and Germany by the 1950s [Smith(1958), Sawyer(1957)]. Although the exact year of development is not known, some evidence suggests that the tests may have been developed in the 1930s. A description of these tests together with a brief history is given in Appendices U2.9 (Germany), U2.10, 2.11 (USA).

In the earliest form of this test (Appendix U2.10), an area confined by a circular steel band was packed full with 62 x 25mm diameter steel balls, which were made to revolve under load by a rotating overhead motor driven disc. Later the test was modified by substituting some of the bearings with a central disc, which had the effect of making the balls run more to the outside perimeter. This test appears to have been the forerunner of ASTM C779-82 Proc C (described in appendix U.2.12), where the balls orbit in a very clearly defined path. This 1982 ASTM test was soon after adopted by the Perth City Council, except that a standard commercial hand-drill mounted upright in an accessory drill-stand was used for driving the race-way.

Rourke(1986) reports that in August 1983 the Concrete Masonry Association of Australia (CMAA) reformed its paving committee to consider the production of design aids for industrial pavements which were trafficked by vehicles with axle loads higher than those permitted on roads.

At the same time, CMAA members were aware of the proliferation of specifications being produced by local government authorities which covered aspects of paving which were not specified in the interim specification MA15(1980) in use at that time. It was decided that a new product specification should be produced.

After some three years of research, testing and debate the aspects of the paving units which were incorporated in the final document: MA20(1986) 'Specification for Concrete Paving Units' were:

- a. tolerance on dimensions
- b. compressive strength, and
- c. abrasion resistance.

The determination of a satisfactory method of specifying an abrasion test procedure and limits proved to be the most difficult section of all the work undertaken in the preparation of MA20.

As a starting point, CMAA conducted a world wide review of abrasion test procedures and catalogued some 32 standard procedures and testing rigs in use throughout the world which may have had applicability to paver testing. In sifting through these tests the CMAA decided on the following selection criteria.

The test should be:

- a. fast enough to allow it to be used as a method of production control
- b. carried out with relatively inexpensive and portable equipment
- c. reproducible and inexpensive on a test-by-test basis
- d. the same as, or similar to existing tests so that results can be compared.

Finally the Perth City Council test was chosen, and experience has shown that this test meets the above criteria very well. Following an experimental study by Shackel(1985)

some refinements to the test procedure were made, and the test was finally incorporated into MA20(1986) as the abrasion test.

The results of the tests revealed that the depth of penetration of the balls into the blocks approximated to the square root of the revolutions of the ball race. i.e. $P = \text{constant} \times (R)$

Thus an abrasion index I_a , was expressed as:

$$I_a = \sqrt{R} / P \dots\dots (9-1)$$

R = revolutions in thousands

It is immediately evident that for a given number of revolutions, the abrasion resistance, I_a , is inversely proportional to the depth of penetration. (Expressing abrasion resistance as the inverse of penetration is both simple and meaningful, and it is possible to do this for most abrasion tests).

The next step in the development of this test was an attempt to correlate factory quality control abrasion tests done on 28-day old pavers, with the visually assessed wear on pavers from the respective factories. The various pavers had been in service for several years at 14 sites across the country.

Thereafter interim limiting criteria were proposed:

$I_a = 2.0$	for heavily trafficked pedestrian pavements
$I_a = 1.5$	for public roadways, and industrial hardstands subject to vehicular slewing loads
$I_a = 1.2$	lightly trafficked areas

In subsequent years these limits were much criticised, since it was noticed that pavers that complied with them did not always perform adequately. Consequently, the indices never moved beyond the status of 'interim'. Notwithstanding, both the test and the limits were widely used even as late as 1996 [Humpula(1996)].

Although the MA20 meets virtually every requirement of an ideal abrasion test, it has one serious drawback, a high variability. This aspect was carefully investigated by Shackel(1992) and is considered in more detail further on in this chapter. Eventually, tests were done to compare the variability of MA20 with a test that had been used by the Sidney South Council, known as the SSC test. This test involved steel balls tumbling/rolling over the face of pavers that were mounted to a revolving box. [Interestingly a very similar test to SSC is used by SABS (SABS 541-1971) and this test was recommended by the CMA, as early as 1983, for abrasion testing. However when the official paving specification SABS 1058 was published in 1985, no abrasion test was included, and what little abrasion testing was being done in South Africa came to a virtual standstill. One possible reason for the exclusion of the SABS test is that the duration of the test was 24 hours, whereas by using bigger balls one hour suffices for the SSC test].

In 1997 the MA20 test was superseded by 'AS/NZS 4456.9' (see appendix U.2.3). This test is clearly based on the SSC test.

9.4 Wear Mechanism of MA20 Abrasion Test

In chapter 4 of volume 2, 66 abrasion tests have been analysed in terms of three dominant mechanisms that lead to abrasion wear, i.e. rolling, impact and sliding. It will be useful to analyse the abrasion mechanisms of the MA20 test under these same headings.

9.4.1 Rolling

It is very apparent that the action of the MA20 abrasion test is that of steel balls rolling under a predetermined load. This results in compressive stresses that result in a gradual but progressive microscopic crushing of the asperities (high points).

In order to arrive at an understanding of the way the balls work their way into the specimen under test it will be useful to magnify the two surfaces that come into contact with each other, i.e. the steel ball of diameter 15.83 mm and the surface of the concrete block. To the human eye a steel ball bearing appears to be very smooth, and this is undoubtedly the reason that the wear pattern induced by the balls on the surface of the block, that of a circular groove, appears to be very smooth as well. However, according to Hutchings(1992), 'all solid surfaces are found to be uneven when studied on a sufficiently fine scale'. Therefore if the two surfaces were to be sufficiently magnified, neither would be smooth. This is illustrated in figure 9.1 below.

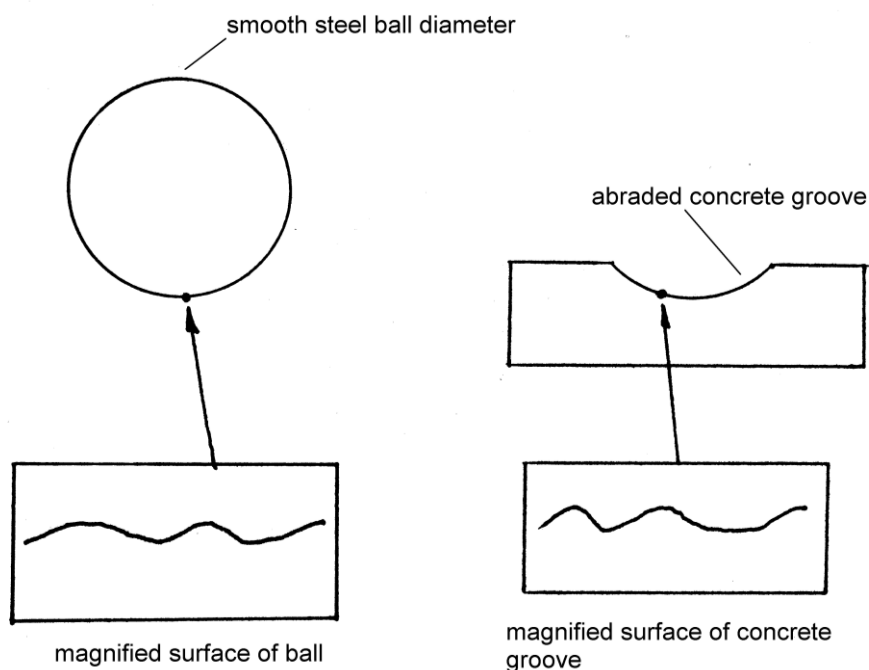


Figure 9.1 Microscopic surface texture of ball and groove

When these two surfaces come into contact with each other, the protruding peaks of the ball will 'crush' the surface of the concrete. The concentration of loading at these points significantly increases the compressive stresses resulting in localised crushing, albeit on a microscopic scale. This is demonstrated diagrammatically in figure 9.2 below (see also figure U.2.12.5 in appendix U):

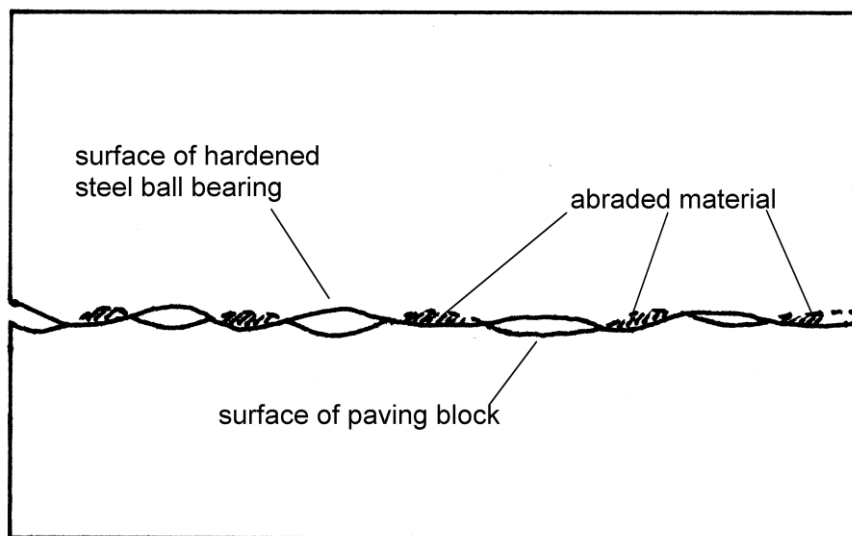


Figure 9.2 Localised crushing of concrete by steel balls - microscopic presentation of MA20 test surface

On such a microscopic scale as illustrated in this diagram, the concrete perceives the ball bearing as a planar surface with microscopic 'hills' and 'valleys'. Note that in reality they are 'rarely steeper than 10 degrees' [Hutchings(1992)].

Although the wear caused by a single pass of one ball is 'infinitesimal', after 5000 revolutions of the drill, each of the balls has moved a distance of:

5000 revolutions of drill shaft = $5000 \times (0.0751 \times \pi) = 1180 \text{ m}$. The end result is a noticeable groove generally ranging between 1 mm to 3 mm in depth.

Other authors have also recognised crushing effects as a primary cause of abrasion:

Robertson(1991) states that 'MA20 is likely to involve crushing of aggregate and paste subject to direct rolling compressive loads'.

TR34(1994) explains that abrasion is essentially due to a 'crushing breakdown' of the surface matrix by high contact pressure.

Severity of Rolling

The principle of the MA20 test may be described as 'loaded revolving steel balls'. The rate of penetration is clearly a function of the contact area. The very high compression at the commencement of the test is a direct result of a small initial contact area. Although an apparatus weighing 17kg does not appear to be heavy, when this force is concentrated at the ball bearing contact points, compressive (and tensile) stresses may exceed the strength of the concrete. This explains why the wear duration curve at the beginning is relatively steep. (This aspect is discussed in greater detail in 9.5.1).

Furthermore, in chapter 3 of volume 2, it is shown that a high spherical load leads to 'Hertzian cone cracks', and probably also 'lateral' and 'axial' cracks. (The Hertzian model is very applicable to the MA20 test since both involve spheres under load). These effects undoubtedly also form part of the localized crushing process. Rolling may therefore be characterised as very 'severe' in the initial phase of the test, tending towards 'mild' with increasing penetration. The former results in the various forms of cracking mentioned

above, occurring over virtually the full contact area (which is very small at this stage), while the latter is limited to the crushing of the asperities, but over a relatively large contact zone.

In table 4.5 of volume 2, rolling is considered to cause severe abrasion, but the associated cracking effects are expected to be shallow (for sub-asperity cracking, and especially for asperity cracking). These aspects are covered in greater detail in chapter 3 of volume 2.

Relevance of MA20 wear mechanism

A common source of localised crushing would be a grain of sand trapped between the heel of a pedestrians shoe and the paving block, which would result in high localised compressive stresses. For example if a man of mass 70 kg steps on a pebble of diameter 4 mm (see figure 9.3 below), and assuming the actual contact area between the pebble and paving block is only 1 mm², then the actual stress transferred to the block is 686 MPa, which far exceeds the strength of even the strongest concrete. It follows that localised crushing will take place at this point of contact and both the paving block and the pebble of sand will be abraded. Similarly any grit trapped beneath the wheels of vehicles will result in similarly high but very localised compressive stresses resulting in abrasion.

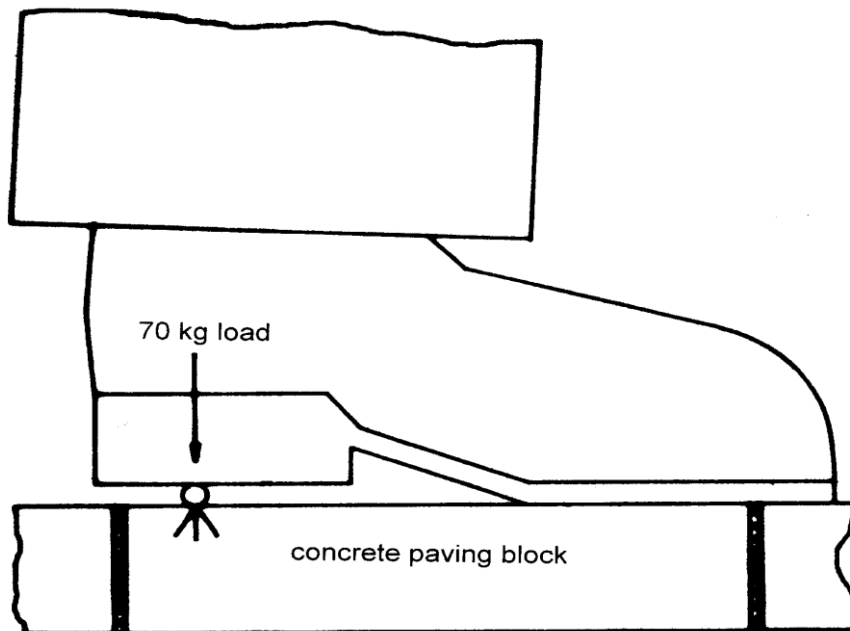


Figure 9.3 High localised crushing induced by pedestrian traffic

Alexander(1984) recommends that the ASTM C779 (Proc. C) test (from which the MA20 is derived) be used for concrete roads subject to heavy steel and track vehicles where grit may be present and for concrete floors subject to heavy applications such as heavy racks.

The hardness of the abrasive grit relative to the paver's surface largely determines the rate of abrasion wear. Hutchings(1992) observed that 'it is observed experimentally that abrasive grit particles of any shape will cause plastic scratching only if the ratio $H_{\text{grit}}/H_{\text{surface}} > 1,2$ I.e. the grit must be at least 1,2 times harder than the concrete surface before any significant scratching effects will occur. This ratio forms the divide between soft and hard abrasion, the latter resulting in abrasion wear that may be several orders of magnitude more. For example Jackson(1924) did abrasion testing with heavily loaded rubber and chained wheels. The wear associated with the former was negligible relative to the latter.(The property of hardness and its various ramifications is carefully considered in chapter 3 of volume 2).

Sectional Conclusion

It may be concluded that abrasion wear in trafficked surfaces is driven almost entirely by hard particles beneath either tyres or footwear, whereas clean concrete surfaces trafficked by leather or rubber will show virtually no wear. Not only are these materials significantly softer, and therefore unable to scratch the concrete, but they are also relatively flexible and thus the contact area is so much greater, resulting in even lower stresses. It is also possible that the very slight abrasion that may occur in clean pavers subject to leather and rubber loads may be more attributable to adhesion than compression related failure. Finally, it should be observed that the ability of the MA20 test to simulate the high compressive stresses that occur beneath a piece of grit or sand under traffic, means that its 'mechanism of wear' is most relevant.

9.4.2 Impact

The microscopic 'crushing' effects described in 9.4.1 may also be produced by impact. In this case kinetic energy inherent in the drill/balls system is imparted to the face of the paver, resulting in wear. The mass of material that is abraded will be a function of the velocity of the drill at the point of impact, U , the mass of the drill, m , and the density and hardness of the concrete [ρ and H], and according to Hutchings(1992) may be expressed as:

$$\text{Mass of material removed} = K \cdot \rho \cdot m \cdot U^2 / (2 \cdot H) \dots\dots (9-2)$$

where K is a dimensionless factor that indicates the fraction of material that is removed as debris for a given strike.

Kinetic energy within the drill/balls system, represented by the $m \cdot U^2/2$ component of equation 9-2 is imparted in three ways:

- (a) **Vibration:** A degree of vibration is noticeable during the test, even at the start of the test. This comes from the internal workings of the motor. As shown in expression 9-2, the downward velocity associated with such vibration will determine how much kinetic energy is imparted.
- (b) **Undulation:** The aggregate component, particularly the coarser particles, is likely to abrade slower than the paste component. It is therefore possible to obtain a circular track that becomes more and more undulating as the test goes on. This will cause some bouncing. As for 'vibration' the amount of kinetic energy imparted will depend on the velocity at the instant of striking.
- (c) **Linear and angular velocity:** The speed of rotation of the drill shaft at 1000 rpm means that the individual balls are rolling a distance of 3,93 meters per second, and this means that each ball revolves 79 times per second, or 4753 rpm. (To have some appreciation of how fast this is, a standard three-phase four-pole induction motor revolves at 1440 rpm at a supply voltage of 380 V.) A microscopic asperity on the concrete's surface will perceive such linear and angular velocities as a huge steel ball rolling/advancing at great speed striking all protrusions in its pathway.

A steel ball impacting on an asperity will clearly also result in crushing and the associated cracking effects described in 9.4.1. Impact may therefore be thought of as rapid crushing, depending on the magnitude of U .

It may be concluded that velocity related impact results in 'crushing' effects in much the same way as compression related 'rolling'.

A number of authors have acknowledged the impact aspect of abrasion wear:

Alexander(1987) makes reference to the abrasive action of the MA20 test as being that of 'impact' from 'high contact-stress steel balls'.

Candy(1992) states that 'abrasion is an *impact* phenomenon and involves the resilience modulus of the material in its elastic range. In order to rationally model the test to field conditions, surface *impact* pressures in the test should be similar to those in the field'.

Rocha(1994) refers to the 'impact and sliding friction' of the MA20 test.

Severity of Impact

As with 'rolling', impact also varies in intensity. 'Mild' impact may be characterized as causing damage only to the asperities, whereas 'severe' impact results in various types of sub-surface cracking including Hertzian cone cracks, lateral cracks and axial cracks. (See chapter 3, volume 2 for an explanation of these various crack systems). A third and very 'extreme' impact regime occurs on a macro scale from much larger loads, and results in through-block flexural cracks developing followed by the eventual disintegration of the block. An example would be at off-loading zones at harbour docks, where surfaces are subjected to iron ore being dropped on them by the off-loading rigs of ships. Fortunately applications involving extreme impact, are not commonplace.

It may be concluded that impact abrasion in MA20 is related to the mass and especially the velocity of the abrading medium. However, while the mass of the apparatus is considerable (17kg), its downward velocity is minimal given the short length of bounce/vibration induced fall, estimated at less than a millimetre. In table 4.5 of Volume 2 the impact abrasion is therefore described as 'mild' in terms of sub-asperity cracking, but is judged to result in major crushing of asperities. Overall the impact of the MA20 test may be therefore be considered as 'mild'.

Sectional Conclusion

In conclusion, a number of words can be used to describe the mechanism of wear in the MA20 test, such as grinding, polishing, impact and especially rolling, but in the final analysis these actions all result in crushing effects, initially at sub-asperity level, soon followed by purely asperity crushing, that result in the loss of material.

9.4.3 Sliding

Two types of sliding may be identified in the MA20 test that will lead to sliding abrasion. These are referred to as Reynolds slip and Heathcote slip. They are described in some detail in 4.2.1(a) and (b) of volume 2. Briefly Reynolds slip occurs as the ball is pushed into an elastic surface. The dome created by pushing the ball into the surface has a greater surface area than the unstressed surface, and in the process some interfacial sliding must occur. For stiff materials such as concrete Reynolds slip contributes very little to abrasion wear. Heathcote slip, on the other hand, accounts for a considerable amount of interfacial sliding, particularly as the depth of the groove increases. Interfacial sliding is inevitable since the circumferential contact between ball and groove is less at the edge of the groove than at the centre.

In conclusion it may be said that sliding abrasion, while certainly present in the MA20 test, is not the dominant mechanism, and this is indicated by assigning to it a 1 in table 4.1 of volume 2, indicating that the shearing action is relatively 'minor'.

9.4.4 Attack on Aggregate/Paste Bond

Figure 9.A shows an aggregate particle nestled into a relatively soft sheath, approximately 50 microns thick, encapsulated by a relatively hard paste of CSH compounds. This sheath generally has a lower b/w ratio due to some entrapped bleeding water beneath the aggregate, and it contains a relatively high proportion of weak CH crystals, which have preferential fracture planes that are orientated parallel to the aggregate particles.

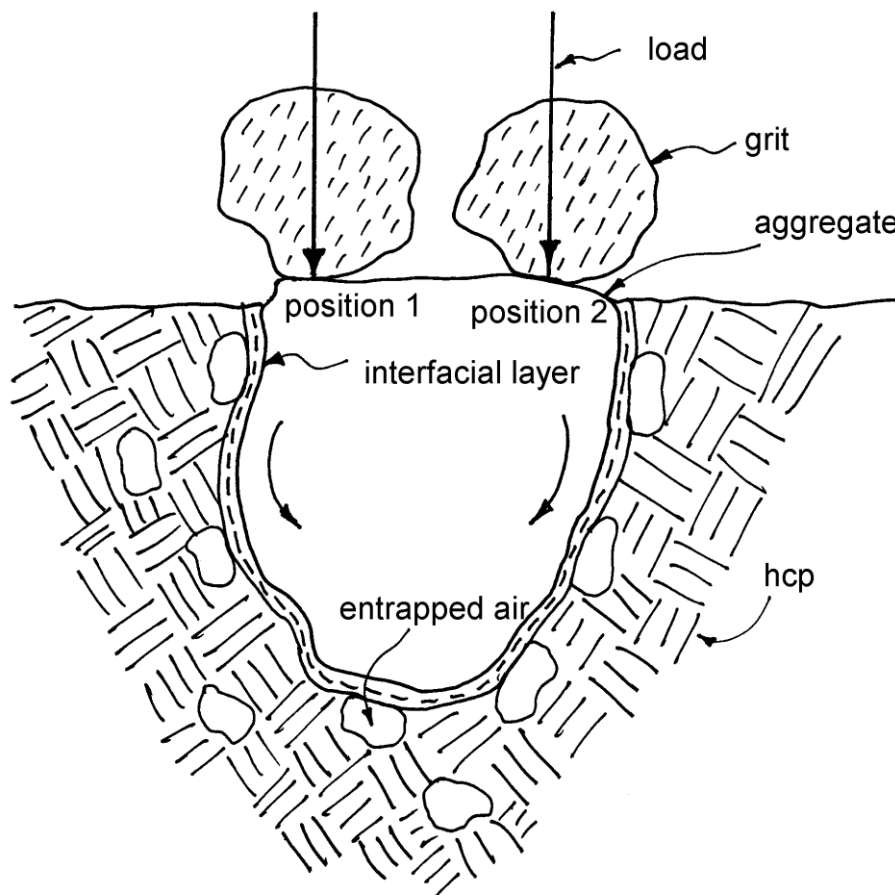


Figure 9.A Aggregate particle nestled in a relatively soft interfacial zone is subject to rocking movements that in time result in de-bonding and dislodgement

When the load is in position 1, the aggregate particle is rotated in a clockwise direction. Later on, as another load is applied in position 2, the particle will rotate anti-clockwise. There will also be a downward movement each time the particle is loaded, and likewise an upward movement on unloading. In the course of time these movements will lead to fatiguing and the aggregate particle and hardened binder paste will de-bond within the interfacial layer. Eventually, with ongoing agitation, the aggregate particle will be dislodged. As pavers are typically made with a b/w ratio of around 2.7, they do not suffer much bleeding, but are sensitive to the affects of limited lubrication. The sketch shows how this results in considerable entrapped air. Generally pavers made with a low binder content, or with too little water, will have a relatively high air content that substantially weakens the binder as well as the binder/aggregate bond.

Sukandar(1993) did abrasion tests using ASTM C779 Proc C ball bearing test (similar to MA20) on a/c ratios ranging between 3 and 9. The a/c = 3 pavers were improved relative to a/c = 9 pavers by 10% in density, 96% in compressive strength, and 233% in abrasion

resistance (where abrasion resistance was taken as the inverse of the rate of penetration after 5 minutes). It is therefore clear that abrasion resistance is far more sensitive to entrapped voids than is compressive strength.

The model shown in figure 9.A offers an explanation for how this can come about. In the case of compression testing the aggregate particles will compress the weak interfacial zone, but compressive loads will still be supported. However in the case of the abrasion test, the aggregate particle may be dislodged once de-bonding has taken place.

Sectional Conclusion

The mechanism of wear in the MA20 abrasion test is ideal in that it simulates 'real' wear in a number of ways:

- 1 It has all three elements of abrasion, i.e. rolling, slipping, and impact. These variously represent the elements of crushing (associated with various forms of cracking) and shearing.
- 2 It simulates the high crushing effects that occur beneath a grain of sand under traffic, which is considered to be the primary cause leading to rapid abrasion.
- 3 It is a very sensitive test, and has a noticeable response to any decrease in density.

9.5 Expressions for MA20 Laboratory results - September 1987

The results of the MA20 laboratory tests can be expressed in two ways; firstly in terms of the depth of penetration of the balls into the block (see 9.5.1), and secondly in terms of the volume of material that was abraded from the groove (see 9.5.2). These two methods are examined and compared in this section, in a qualitative sense, while various abrasion indices are qualitatively compared in section 9.6.

9.5.1 Expressing MA20 results as a function of depth

The simplest possible way of expressing the results of the MA20 test is by defining abrasion-wear as the depth of the groove after a given number of revolutions, usually after 5000 revolutions. For the various test specimens, the penetration of the balls have been recorded after 1000, 2000, 3000, 4000 and 5000 revolutions, and the results are shown in appendices J.1 through J.8.

The results are also shown graphically in eight wear vs duration curves recorded in appendices J.17 through J.24. For the purpose of discussion Figures 9.4, 9.5, and 9.6 are reproduced below from these appendices to show the variations that can be expected from rich, normal and lean mixes.

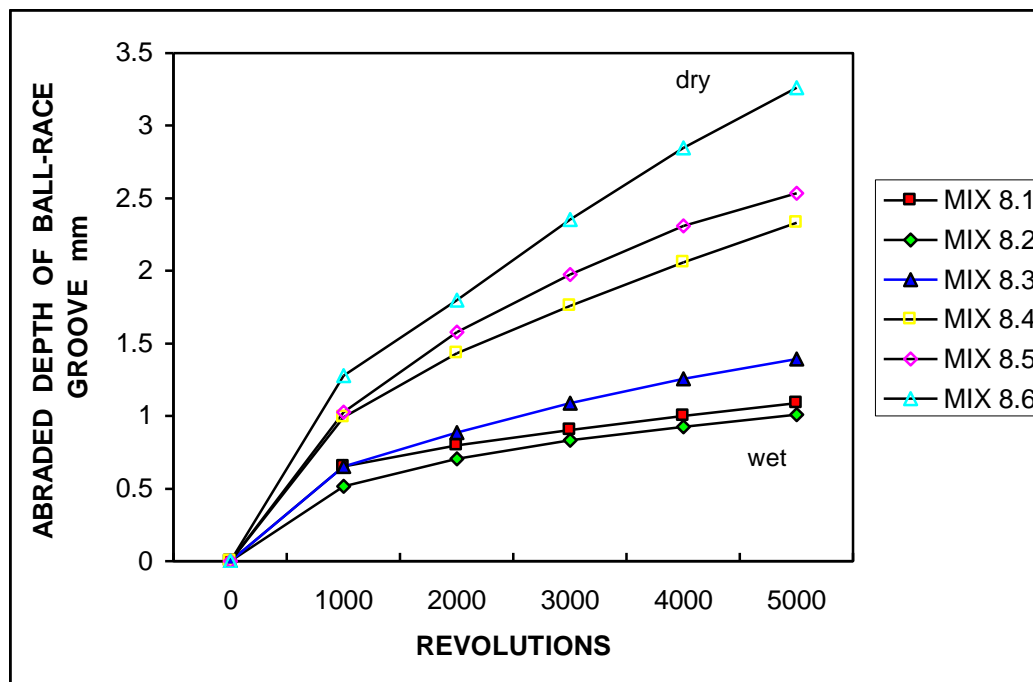


Figure 9.4 Relationship between depth of wear and revolutions of race-way
Mix 1 : 9% OPC, 9% MGBS

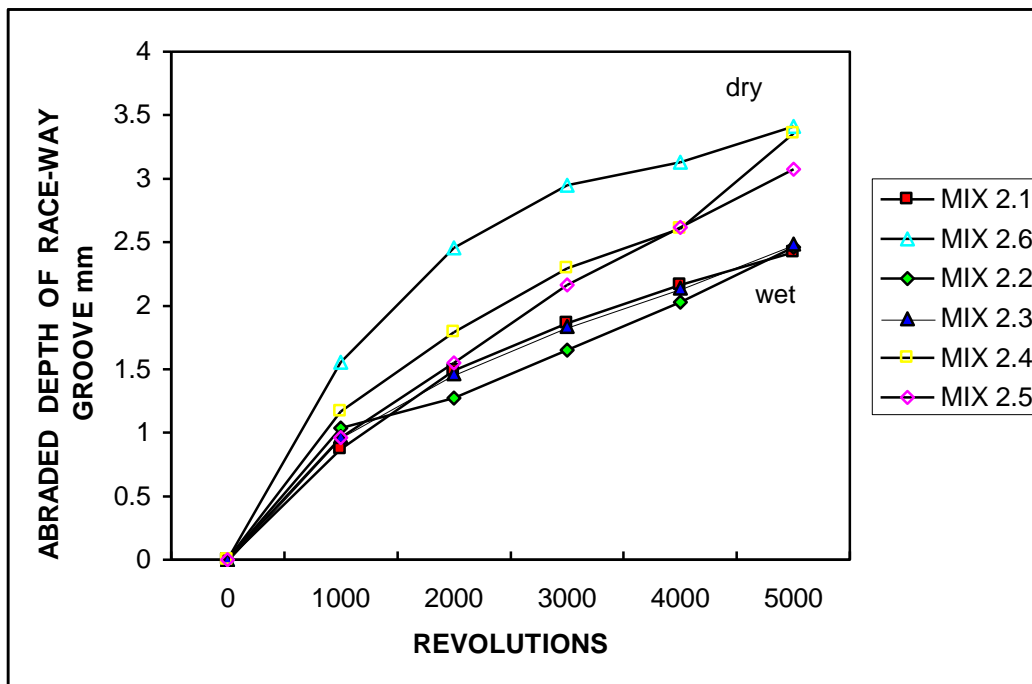


Figure 9.5 Relationship between depth of wear and revolutions of race-way
Mix 2 – 7% OPC, 7% MGBS

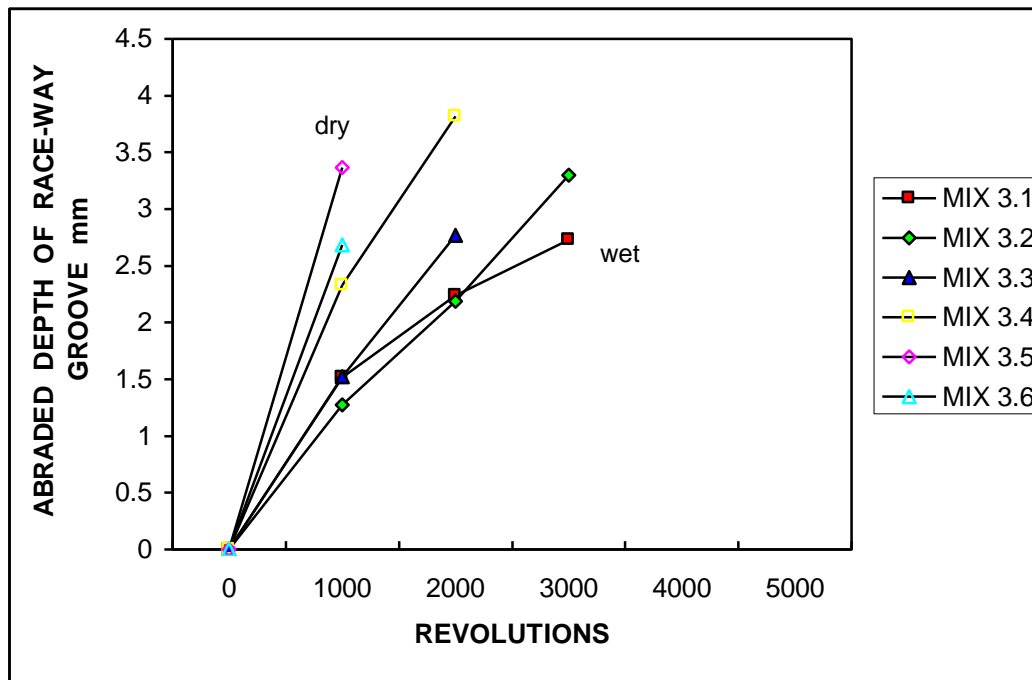


Figure 9.6 Relationship between depth of wear and revolutions of race-way
Mix 3 – 5% OPC, 5% MGBS

Observations from the graphs

The graphs illustrate the typical relationship between depth of wear and abrasive effort or revolutions.

All three figures show that the penetration of the balls is significantly less for 'wet' mixes. This is because the extra water in the wet mixes facilitates compaction and hence greater density. This principle is fully discussed in chapter 6.

The graphs also show that binder content plays an important role. Blocks with 18 % binder content (figure 9.4) have significantly shallower penetrations compared to blocks with 14% and 10% binder (figures 9.5 and 9.6).

A feature of the lines in these figures is that they decrease in gradient as revolutions increase, and this is characteristic of the MA20 test. The most obvious reason for this is that the contact surface area between balls and block increases as the depth increases, with a corresponding decrease in contact stress. It follows that the lower the stresses are on a macroscopic level, the lower will be the stresses on the microscopic peaks between balls and block and hence the slower rate of asperity crushing as depth increases.

Macroscopic stresses

Consider figure 9.7 to better understand the 'macroscopic' stresses that result in an abraded section resembling a segment of a circle.

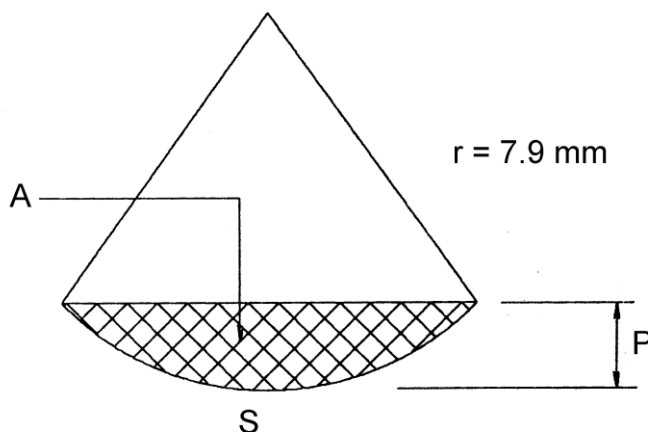


Figure 9.7 Typical cross section of MA20 abrasion groove

where:

$$\begin{aligned}
 P &= \text{depth of wear (read from dial gauge)} \\
 S &= \text{arc length} \\
 &= 2r \cos^{-1}(r-P)/r, \quad [(r-P)/r \text{ in radians}] \quad (9-4)
 \end{aligned}$$

$$\begin{aligned}
 C &= \text{Compressive Stress} \\
 &= 17\text{kg} \times 9.81 / (13 \text{ balls} \times 0.5 \text{ mm} \times S) \quad (9-5)
 \end{aligned}$$

From the expression for S in equation 9-4, it is possible to plot the relationship between depth (P), and contact arc length (S), as in figure 9.8. The effect that this has on the compressive stress (C), is shown in figure 9.9. A contact length of 0.5 mm has been assumed between ball and groove in the direction normal to S. In plotting figure 9.8, it was necessary to use penetrations corresponding to R_{1000} , R_{2000} , or R_{3000} rather than R_{5000} in some of the weaker mixes e.g. those shown in figure 9.6.

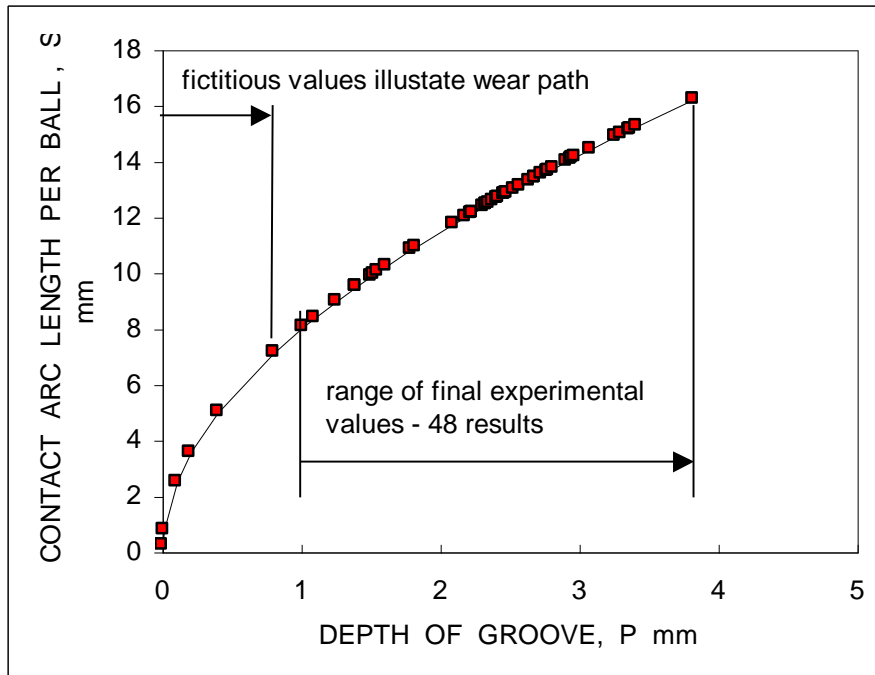


Figure 9.8 Relationship between Contact Arc Length and Abraded Depth

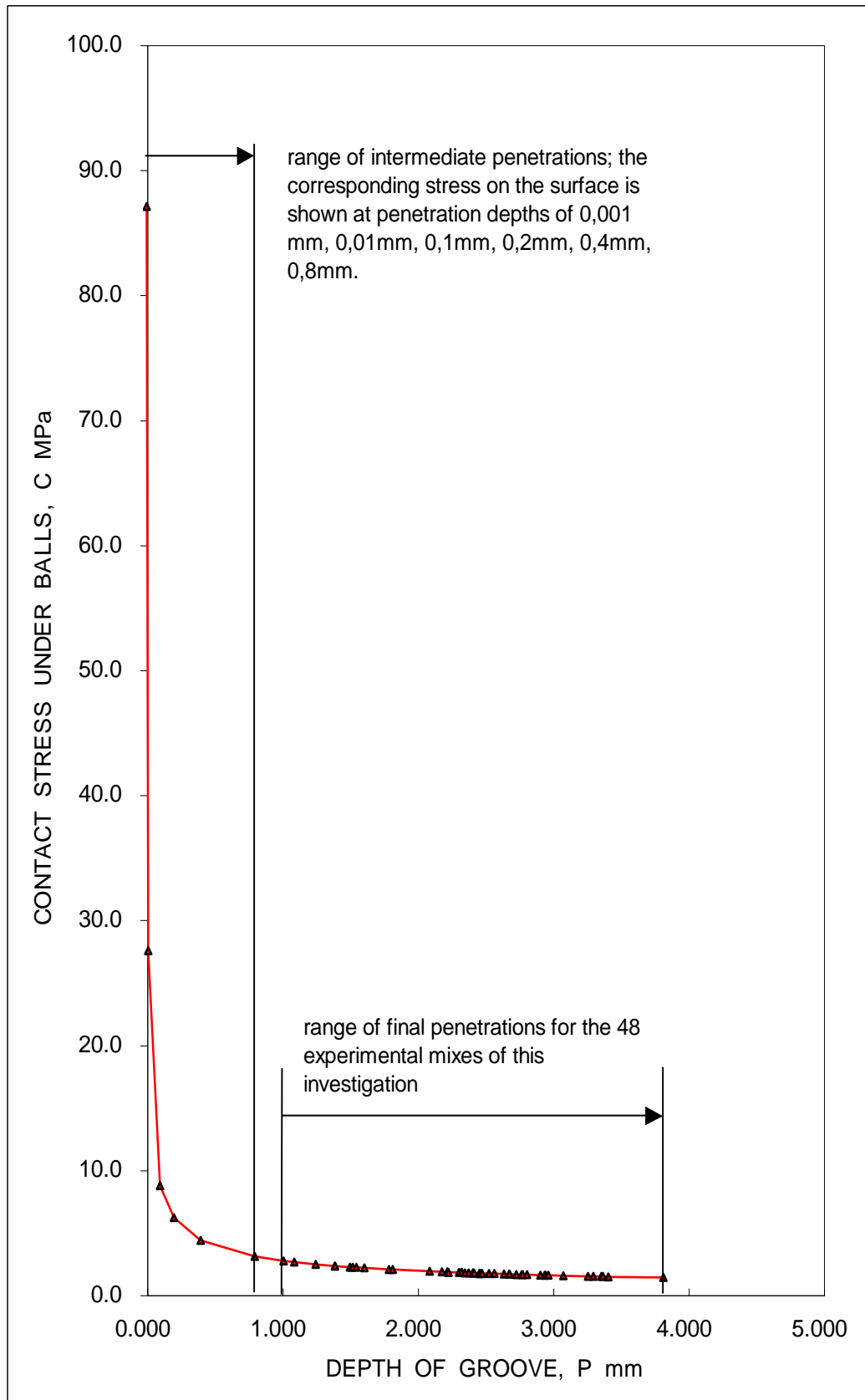


Figure 9.9 Relationship Between Compressive Stress and Abraded Depth

Figure 9.9 shows very high stresses at the start of the test, of the order of 90MPa. This explains why all the wear-duration graphs for all the mix designs e.g. figures 9.4 through 9.6 show a rapid rate of penetration for the first 1000 revolutions, and it is likely that the bulk of *this* wear occurred in the first 100 or 200 revolutions.

The mechanism of wear for the first 100 revolutions will likely correspond to some sub-asperity cracking, rather than the more mild asperity crushing after 1000 revs. It is evident that by the time the 5000 revolutions were completed the depth of wear was 1mm or more for the 48 mixes (according to figure 9.9), and hence the compressive stresses were 3 MPa or less. It follows that with such low stresses continued crushing is only possible by concentrating the load at asperities.

Other investigators [Smith(1958), Tangtermsirikul(1997)] have used ball-under-load tests based on the principle of the balls not being confined to a particular track as they move over the surface. In this case the surface abrades evenly all over, and the rate of penetration, all things being equal, is nearly constant. This was confirmed by the results of both these authors.

The advantage of this is that a higher initial penetration is far easier to interpret as inadequate curing, or a weak topping, etc. Alternatively, a lower penetration rate may be the result of some hardening having taken place, e.g. carbonation, or an effective liquid surface treatment. Conversely the ever changing contact arc length, S , of the MA20 test, and so the ever changing stress below the balls, makes interpretation more difficult.

9.5.2 Expressing MA20 as a function of volume

Just as it is possible to express the MA20 results in terms of the depth of the groove, P , it is also possible to do so in terms of volume. Once the depth has been measured, it is possible to calculate the cross sectional area of the groove, A , (equation 9-6), and hence the volume of the groove, V , (equation 9-7).

$$\begin{aligned} A &= \text{abraded area} \\ &= r.(S/2-(r-P)\sin(S/(2r))) \quad (\text{with } S/2r \text{ in radians}) \end{aligned} \quad (9-6)$$

$$\begin{aligned} V &= \text{volume of abraded material} \\ &= A.\pi.d \end{aligned} \quad (9-7)$$

$$\begin{aligned} d &= \text{mean diameter of race-way} \\ S &= \text{see equation (9-4)} \end{aligned}$$

Figure 9.10 plots the relationship between depth and volume for the 48 mixes, as well as for some fictitious intermediate values below a depth of 1mm. It may be seen that the volume of the groove is approximately linear with depth in the range 1mm to 4mm. For this reason figures 9.10 through 9.12 are very similar in shape to figures 9.4 through 9.6.

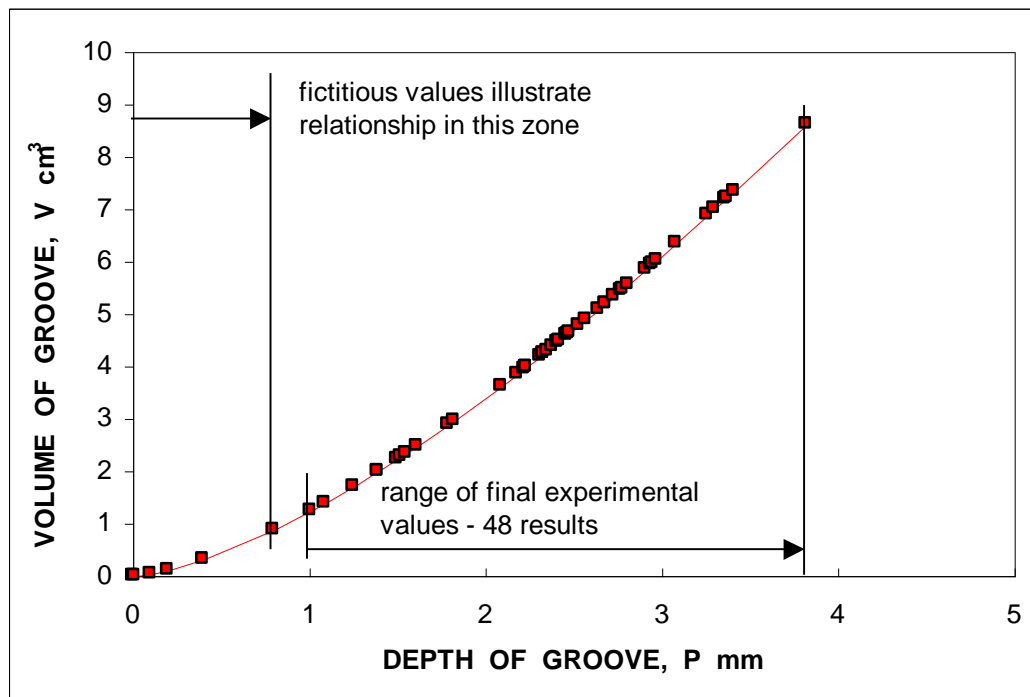


Figure 9.10 Relationship between depth of groove and volume of groove

Appendices J.9 through J.16 record the MA20 results in terms of the volume of the groove.

This information in turn is illustrated in eight volume versus revolutions graphs, recorded in appendices J.25 through J.32.

Figures 9.11 through 9.13 are reproduced from these appendices to show the relationship between volume and revolutions.

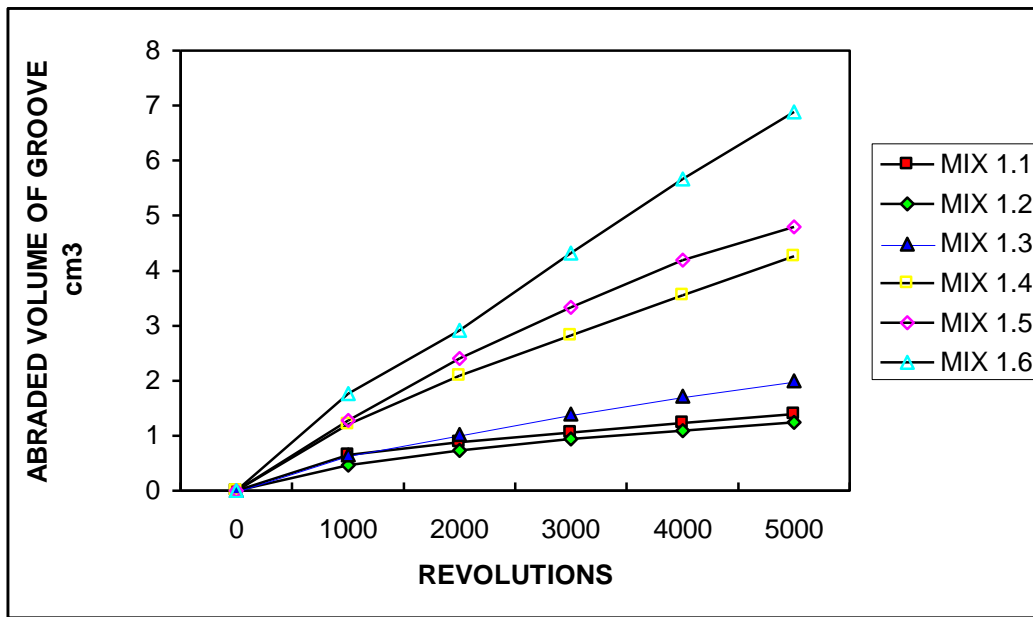


Figure 9.11 Relationship between abraded volume and ball-race revolutions
Mix 1 – OPC 9%, MGBS 9%

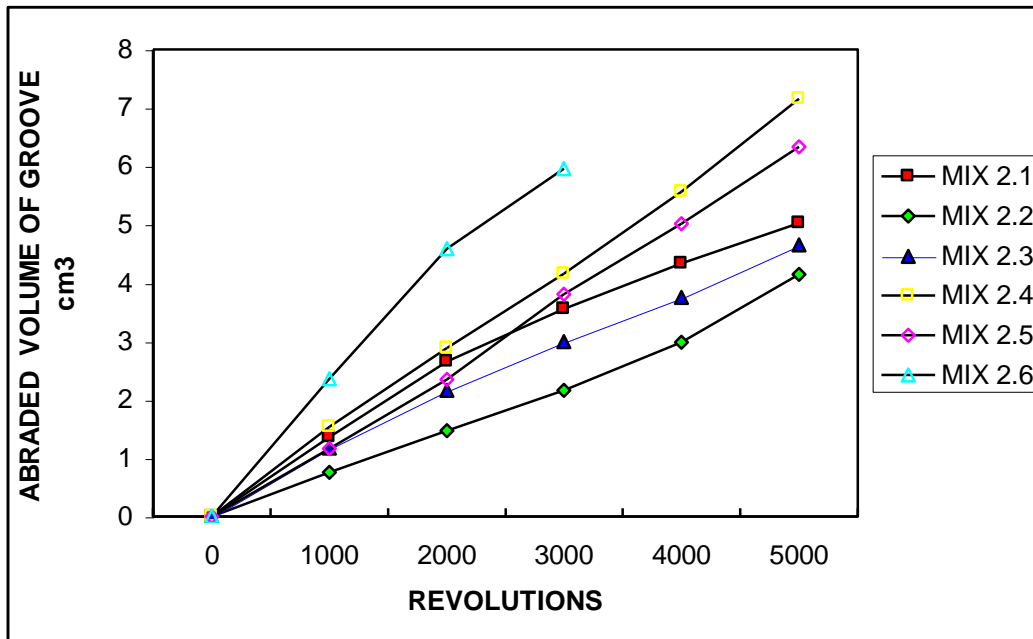


Figure 9.12 Relationship between abraded volume and ball-race revolutions
Mix 2 – OPC 7%, MGBS 7%

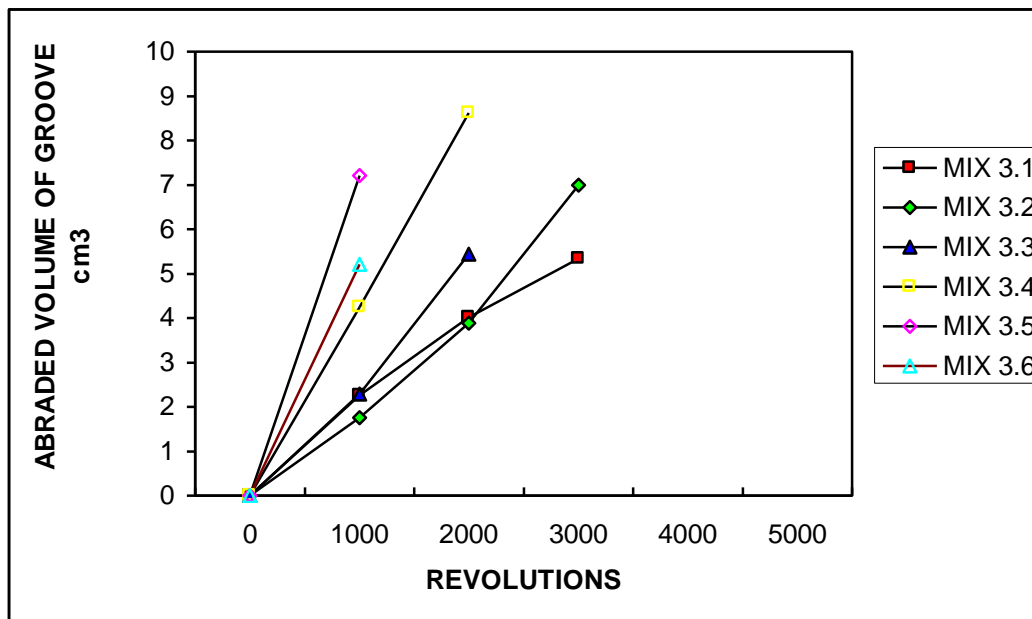


Figure 9.13 Relationship between abraded volume and ball-race revolutions
Mix 3 – 5% OPC, MGBS 5%

9.5.2.1 Advantages of Expressing Abrasion Wear as a Function of Volume

Expressing the MA20 results as a function of volume is useful for a number of reasons:

- It is easier for the man in the street, or even the average manufacturer, or for that matter the engineer to understand the concept of volume, rather than an index that describes a particular shape of a wear duration curve involving a square root and inverse function (as in 9.5.1.1).
- Comparison with other abrasion tests used in this programme becomes a simple matter. (In both the ASTM C418 and wirebrush abrasion tests the recommended way of measuring wear is to fill the abraded zones with plasticine from which the volume of abraded material is then calculated). This would obviate the need to invert the abrasion indices of the ASTM C418 and Wirebrush (clay method) tests before a comparison can be made with the MA20 test, as was done in table 6.15.

A comparison of the three tests on the basis of abraded volume is done in 12.2.12.

[Note that expressing abrasion as a function of depth of wear, as was done in 9.5.12 will also allow for comparisons with the ASTM C418 and the Wirebrush test, since these may be expressed as the volume/area \equiv average depth].

- The shape of the wear duration curve in the case of the 'abraded volume' approximates to a straight line. Comparing figures 9.4 with 9.11, 9.5 with 9.12, and 9.6 with 9.13, the wear-duration curve is more linear when expressed in terms of volume.

The relatively straight lines in the above figures suggest that the rate of material removal is virtually constant (although a higher initial penetration is still observable in figure 9.11). Thus for a given abrasive effort, in this case 1000 rpm of the ball-

race at a constant force, the volume of material abraded per 1000 rpm is nearly constant. Therefore the relatively high compressive stress acting in a small groove for say the second 1000 revolutions results in nearly the same rate of wear as that of a relatively low compressive stress acting in a wide groove corresponding to the last 1000 revolutions. On a microscopic scale it may be said that *fewer* protruding peaks of concrete are crushed *more forcefully* when the arc length is small, and conversely, *more* peaks are crushed *less forcefully* when the arc length is large.

Assuming that the straight lines of the V versus R graphs indicate that abraded volume is directly proportional to abrasive effort, then it should be possible to determine what a surface will look like in five or ten years time, assuming that the wear on site is also linearly related to traffic and providing that a correlation with the abrasion test can be established. This opens the way to predicting the total wear on large areas of installed cbp (see chapter 14 and 15).

9.5.2.2 A theoretical model of wear in terms of volume

Archard(1953) developed an equation that states that the volume of abraded material is directly proportional to the product of the applied normal force and the sliding distance and inversely proportional to the surface hardness.

$$Q = K.W.S/H \dots\dots (9-8)$$

Where:

- Q = volume of abraded material
- W = the applied force
- S = the sliding distance
- H = the surface hardness
- K = a dimensionless wear coefficient that indicates the severity of the wear process in different systems (i.e. different materials, different abrasives, etc.). K may be considered as the probability of each asperity interaction resulting in the production of a wear particle.

This model is based on the plastic deformation that occurs as a hard surface *scrapes over* a softer counterface, and has been found to be a good predictor of plastic wear in both metals and ceramics. Note that by using a different approach an identical expression can be developed by assuming a hard protuberance *cutting through* the counterface [Hutchings(1992)]. These aspects are discussed in greater detail in 3.4.4 of volume 2.

Although Archard's model refers specifically to wear associated with plastic deformation, it may be argued that part of the micro crushing process of a concrete surface, as it occurs in the MA20 test and in several applications, involves a transition from purely elastic to plastic behaviour. Furthermore, such plasticised material in the MA20 test is subject to sliding via the mechanism of Heathcote slip. These conditions fit the requirements of Archard's equation.

Other abrasion tests also fit the Archard model. There are at least five countries in Europe that make use of the Amsler abrasion machine to do abrasion testing; Germany, Belgium, Spain, The Netherlands, and Austria (see appendices U.5.2 , 5.3, 5.4, 5.8, 5.9). However none of them use the same limiting criteria in terms of the pressure applied to the specimen and the total revolutions. V d Klugt(1989) stated that the various tests are nevertheless comparable, since abrasion is directly proportional to sliding distance, and a function of (though not necessarily directly proportional to) the applied force. In effect this is equivalent to stating that Q is proportional to S and to W^x , in close agreement with expression (9-8).

Bowden(1964) reported that even though the types and properties of non-metallic materials show a wide variety, the wear mechanism may generally be expressed with the wear laws given in expression (9-8) above for metals.

Earlier it was seen that the linearity of the wear-duration curve of the MA20 test, whether measured on a volume or depth basis, is not as good for the first 1000 revolutions as from 1000 to 5000 revolutions. It was suggested that the very high stresses at the start of the test resulted in localised crushing that may go beyond the 'microscopic-asperity' realm to a sub-surface level; hence the higher rate of volume loss.

On the other hand where these high initial stresses are unlikely to be encountered, such as in surfaces free of grit/sand, a formula for wear in terms of volume loss can be formulated for the MA20 test as follows:

$$V = n \times R \dots\dots\dots(9-9)$$

Where:

V = volume of abraded material

R = revolutions of ball-race

n = the constant. This is the slope of the line, and is steeper for dry mixes with low cement contents and conversely shallower for wet mixes with high cement contents.

A very similar expression for actual wear on site can be formulated as:

$$V = \text{Constant} \times \text{abrasive effort (pedestrians or vehicles)}$$

This method of expressing abrasion will be analysed in some detail in 9.6.3.

Expression 9-9 may be seen to be merely a simplification of (9-8), except that in (9-9) H and W are assumed constants and therefore built into the constant n. Thus Archard's equation is a useful model for the MA20_{volume} test.

9.5.3 Sectional Conclusion

This section has considered two ways of expressing the MA20 laboratory results; as a function of depth and as a function of volume.

The mechanism of abrasion wear is briefly discussed and appears to be compatible with the criteria of Archard's equation. Furthermore Archard's equation predicts that abrasion wear in the field will be proportional to both the abrasiveness and volume of the traffic, and inversely proportional to the hardness of the surface. It may therefore be anticipated that a good correlation should exist between MA20 abrasion wear and field abrasion wear. This correlation is the essence of chapter 14.

9.6 Abrasion Indices

In this section six different abrasion indices are considered with a view to determining which one most accurately quantifies abrasion resistance or abrasion wear. The first two indices considered (in 9.6.1 and 9.6.2) relate to abrasion resistance, followed by four others that express abrasion wear.

Thereafter the six indices are correlated with compression testing results. This is justified by arguing that the compression testing results *of this investigation* are closely related to abrasion resistance since (1) the blocks all received the same curing, (2) the same aggregates were used throughout, (3) no special surface finishes were applied, (4) the same production process was common to all, etc. The compressive strength in this instance may therefore be considered a good indicator of both core *and* surface quality. Therefore the index which correlates best with the compression test may also be considered the most suited for the MA20 abrasion test. Once again, the results of the three crushing test methods are all combined to obtain an 'average-of-18' result, to give the best possible indication of the strength/quality.

9.6.1 I_{MA20} - the Official MA20 Index

The results of the early work conducted in Australia revealed that the depth of penetration of the balls into the blocks approximated to the square root of the revolutions of the ball race. i.e. $P = \text{constant} \times \sqrt{R}$, (R in thousands).

Thus the 'standard' abrasion index I_a could be expressed as:

$$I_{MA20} = \sqrt{(R)} / P \text{ (i.e. expression 9-1).}$$

This is the official abrasion index of the MA20 abrasion test.

The data and computations for each individual block are recorded in appendices J.1 through J.8, while the average result for a mix is based on five tests, and may be expressed as:

$$I_{MA20} = [\sqrt{(R_1)/P_1} + \sqrt{(R_2)/P_2} + \sqrt{(R_3)/P_3} + \sqrt{(R_4)/P_4} + \sqrt{(R_5)/P_5}] / 5 \dots\dots (9-10)$$

The results for the 48 mixes are reported in column C of table 9.2.

Clearly this index is directly proportional to the square root of the revolutions, and indirectly proportional to the penetration. This has two useful implications: (1) For a given number of revolutions, usually 5000, the index I_a , may be considered equivalent to the *abrasion resistance* since expressing abrasion resistance as the inverse of penetration is widely accepted. (2) Where the penetration is only available for a lesser number of revolutions, then the index can still be calculated from 9-10. For example this can happen if the rate of penetration is so high that the locating cage of the ball-race is in danger of making contact with the test specimen, whereupon it will be necessary to stop the test before 5000 revolutions (e.g. see figure 9.6). If the assumption is correct that the depth of penetration of the balls into the blocks is indeed proportional to the square root of the revolutions of the ball race, then the abrasion index at 1000 revolutions will be the same as that at 2000, 3000, 4000 or 5000.

9.6.2 la_{INT} - the Integer Index

These calculations are also recorded in appendices J.1 through J.8. Each 'mean' of five tests (see appendices) represents one of 48 mix designs. They have been summarised in column J of table 6.2, and again replicated in column D of table 9-2. They are widely used throughout this manuscript.

There is a subtle difference between la_{MA20} and la_{INT} . The former is the average of five individual la computations, substituting into expression (9-10) the *individual penetrations* corresponding to the most revolutions (R) for each test. Usually this will be at 5000 revolutions (R_{5000}), but if the test was terminated early, then the average penetration corresponding to R_{4000} , R_{3000} , R_{2000} , or even R_{1000} is used. On the other hand la_{INT} uses the *average penetration*, again usually taken where possible at 5000 revolutions (R_{5000}), but if the test was terminated early, then the *average* penetration corresponding to R_{4000} , R_{3000} , R_{2000} , or even R_{1000} is used. The advantage of using la_{INT} is that an average penetration may be selected where at least four or preferably five penetration readings were recorded for a given revolution. The index is thus based on a known revolution, which will always be a multiple of 1000, and therefore the square root function will always apply to an integer, either 5, 4, 3, 2 or 1. By way of contrast the la_{MA20} index may relate to two, three or even four different revolutions, depending on when each test was stopped (e.g. consider mix 3.2 in appendix J.3, where la_{MA20} is based on penetrations corresponding to R_{5000} , R_{4000} , R_{2000} , $R_{3000} \times 2$, whereas la_{INT} is based entirely on penetrations corresponding to R_{3000}).

la_{INT} may be expressed as:

$$la_{INT} = \sqrt{(R_x)/P_x} \dots\dots (9-11)$$

Where,

R_x = [the revolutions at either 5000, 4000, 3000, 2000 or 1000] / 1000

P_x = the average penetration after R_x revolutions

= $[P_{1x} + P_{2x} + P_{3x} + P_{4x} + P_{5x}] / 5$ (in the case where 5 penetrations were measured).

la_{INT} is used in figures 9.14 through 9.16.

Generally la_{MA20} is very similar to la_{INT} , (compare column C and D of table 9-2), but not exactly the same, since clearly expressions 9-10 and 9-11 are distinctly different.

Sectional summary

The abrasion indices considered in this section represent abrasion resistance. In the next sections, 9.6.3 through 9.6.6, indices will be considered that represent abrasion-wear. It should be observed that many abrasion tests quantify abrasion wear rather than abrasion resistance, including two tests used in this investigation, i.e. the ASTM C418 sandblast test and the PCI.TM.7.11 wire-brush test. However it is often possible to convert abrasion-wear to abrasion resistance. If abrasion-wear is expressed in a form where it is directly proportional to the penetration of the abrasive, then the abrasion resistance may be considered as the reciprocal of this, and vice-versa.

9.6.3 The n_{\log} index

It has variously been stated that the MA20 abrasion test assumes that the penetration of the balls into the block is proportional to the square root of the revolutions and may be expressed as follows:

$$P = 1/la \times R \quad (R \text{ in thousands})$$

In a more general form this may be expressed as follows:

$$P = 1/la \times R^n$$

If the equation is expressed in the logarithmic form it takes on the classical straight line expression $y = a.x + b$ as follows:

$$\log P = n \times \log R - \log la \dots\dots(9-12)$$

Where:

- n = slope of the straight line (also referred to as n_{\log})
- $\log la$ = intercept on Y axis
- $\log R$ = log of revolutions of the ball-race in thousands. This value represents the abrasive effort and is the independent variable.
- $\log P$ = log of penetration of the balls into the paver.
This is the dependant variable, dependant on the abrasive effort, R.

From the P and R results recorded in appendix J.1 through J.8, log P and log R values have been calculated for the 48 tests and are recorded in appendices J.33 through J.40.

For each mix, a linear regression analysis tests the degree to which the log P values (corresponding to $\log R_{1000}$, $\log R_{2000}$, $\log R_{3000}$, $\log R_{4000}$, and $\log R_{5000}$) are in a straight line. This analysis may also be seen in appendices J.33 through J.40.

By way of example some of the data corresponding to mixes 1.1, 2.2, and 2.5 have been extracted from these appendices, and are shown in table 9.1. Graphs have been plotted for these mixes (i.e. figures 9.14 through 9.16), and the regression line passing between the $\log R : \log P$ coordinates indicates a high degree of linearity, as do the high R^2 values for all the mixes shown further on in table 9.2.

TABLE 9.1 REGRESSION ANALYSIS DATA FOR THREE MIXES						
MIX	SPECIMEN	LOG P ACTUAL P	LOG P REGRESSION ESTIMATE	LOG R	LOG P For n=0.5 @ la =	
1.1	1.1.1	-0.18708	-0.19045	0	-0.31281183	2.055
	1.1.2	-0.09691	-0.0949	0.301029	-0.16229733	
	1.1.3	-0.04575	-0.03901	0.477121	-0.07425133	
	1.1.4	0	0.000644	0.602059	-0.01178233	
	1.1.5	0.037426	0.031404	0.69897	0.036673174	
2.2	2.2.1	0.017033	-0.01411	0	0.041914151	0.908
	2.2.2	0.103803	0.146206	0.301029	0.192428651	
	2.2.3	0.217483	0.239989	0.477121	0.280474651	
	2.2.4	0.307496	0.30653	0.602059	0.342943651	
	2.2.5	0.390935	0.358142	0.69897	0.391399151	
2.5	2.5.1	-0.01772	-0.02042	0	0.138465589	0.727
	2.5.2	0.190331	0.198829	0.301029	0.288980089	
	2.5.3	0.334453	0.327087	0.477121	0.377026089	
	2.5.4	0.41664	0.418087	0.602059	0.439495089	
	2.5.5	0.48855	0.488673	0.69897	0.487950589	

Figure 9.14 shows the relationship between log R and log P for a strong mix, i.e. Mix 1.1.

Figure 9.15 shows the relationship between log R and log P for a weak mix, i.e. Mix 2.5.

Figure 9.16 shows the relationship between log R and log P for relatively non linear results, i.e. Mix 2.2. (relative to mix 1.1 and 2.5 it has a relatively low R^2 value, 0.952),

In the MA20 abrasion test it is assumed that $n = 0.5$. If the la_{INT} values from appendices J.1 through J.8 are used with this n value, then using expression 9-12 it is possible to calculate the log P coordinates corresponding to $\log R_{1000}$, $\log R_{2000}$, $\log R_{3000}$, $\log R_{4000}$, and $\log R_{5000}$. This is how the co-ordinates for the second line shown in figures 9.14 through 9.16 were obtained. This line allows an immediate comparison with the regression line, and shows the difference between n_{log} and $n_{=0.5}$. (n_{log} is the slope of the regression line passing through the log P : log R coordinates, while $n_{=0.5}$ is a fixed slope that begins at la_{INT} on the Y axis, and passes through the calculated log P ordinates corresponding to the log R values at $R = 1000, 2000, 3000, 4000$ and 5000).

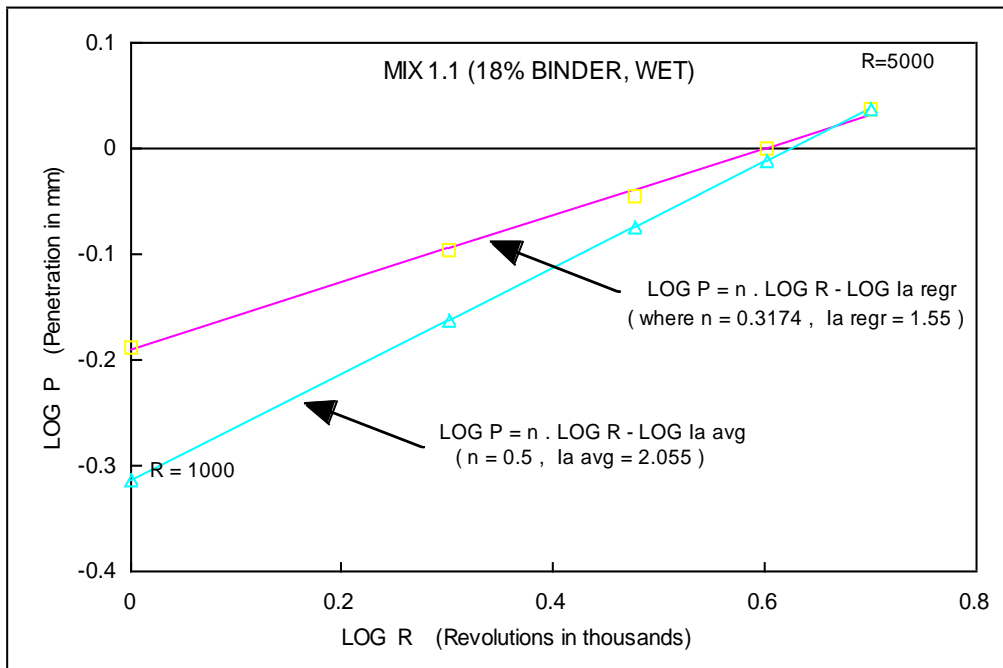


Figure 9.14 Relationship between log P and log R – Mix 1.1

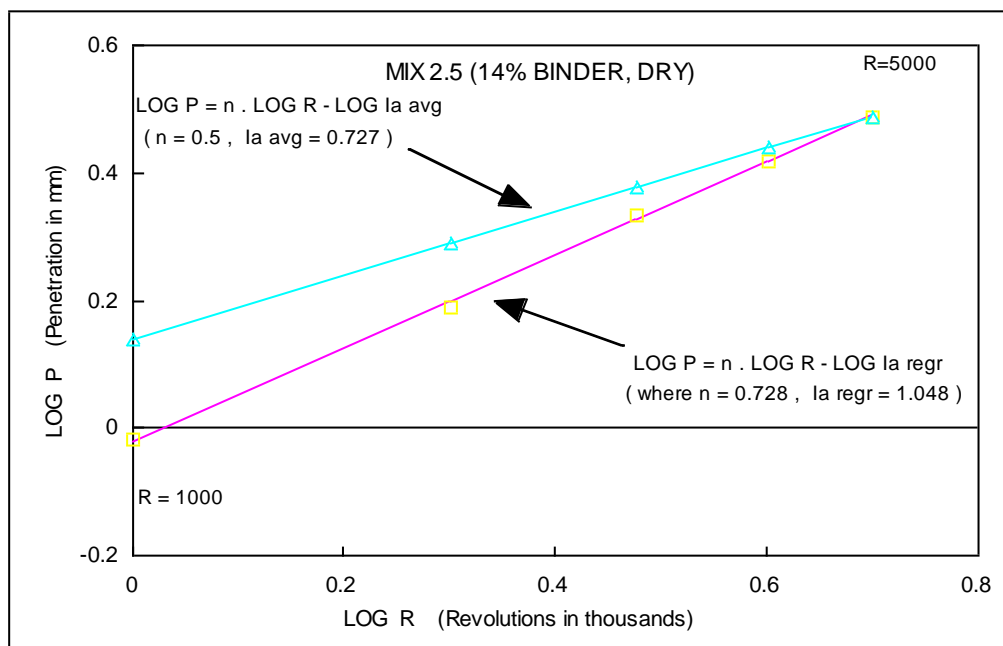


Figure 9.15 Relationship between log P and log R – Mix 2.5

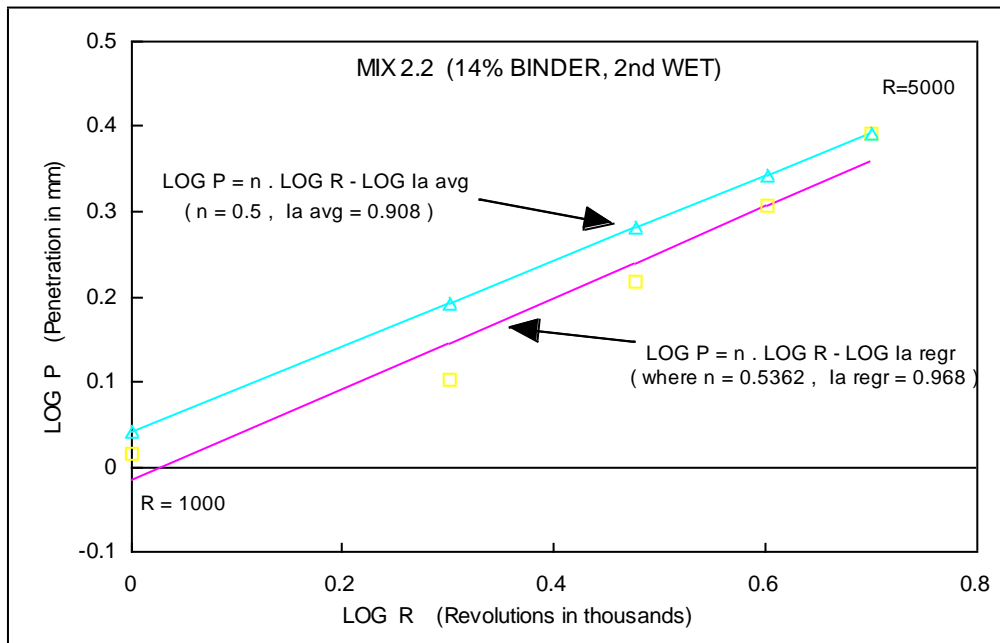


Figure 9.16 Relationship between log P and log R – **Mix 2.2**

Comments

The linearity of expression (9-12) is clearly visible from these figures, even for mix 2.2. I.e. the 'regression line' computed from the 'Regression log P' values in table 9.1 is very close to the actual 'log P' values. R^2 values of 0,98 and 0,99 are typical, as may be seen in appendices J.33 through J.40.

At first glance it would appear that the assumption made in MA20 that $n = 0.5$ is not accurate. Figure 9.14, representing a strong mix, shows $n_{log} = 0,317$. Furthermore figure 9.15, representing a weak mix, has $n_{log} = 0,727$. It therefore seems that for strong blocks n should be less than 0,5, while for weak blocks n should be greater than 0,5.

This suggests that the value of n_{log} , which is simply the slope of the log R vs log P graph, might be a suitable indicator of abrasion wear. Thus:

$$\text{Abrasion wear index} \propto n_{log} \dots\dots (9-13)$$

$-n_{log}$ should not be confused with the abrasion index Ia_{INT} , which indicates abrasion resistance.

In comparing figures 9.14 through 9.16, the difference between Ia_{INT} and Ia_{log} can be seen from the intercepts on the Y axis, while the divergence in the two slopes represents the difference in the regression slope n_{log} , and the $n_{=0.5}$ slope. (It bears repeating that the $n_{=0.5}$ line relates to the slope of a line passing through the calculated P_{1000} through P_{5000} ordinates, while the n_{log} line is the best fit straight line between experimental P_{1000} and P_{5000} ordinates).

Three different indices are referred to here and some clarification is required:

- Ia_{INT} is used in figures 9.14 through 9.16 (and in appendices J.1 through J.8). It is computed from the average penetration of five blocks at 5000 revolutions. However, where a test was terminated early, it is based on the penetration of five blocks at lower revolutions (see 9.6.2 for a full discussion on Ia_{INT}).

- b. la_{MA20} is the official la of MA20. As in la_{INT} , n is always assumed to be 0,5. Generally la_{MA20} is very similar to la_{INT} , but not exactly equal. It is the average of the individual la values corresponding to the *individual* penetrations in each of the five blocks. The individual penetrations may also have different revolutions, particularly where tests are terminated early, and therefore the mean value for la , for a set of five blocks, may not correspond to either 1000, 2000, 3000, 4000, or 5000 revolutions. For plotting graphs this becomes problematic, and for this reason la_{INT} has been preferred to la_{MA20} in this investigation.
- c. la_{log} is also shown in figure 9.14 through to figure 9.16 (from appendices J33 - J 40) and is the intercept of the regression line (the best fit line passing through experimental P_{1000} through P_{5000} ordinates. Note that P_0 is ignored).

Note that la_{log} is a function of the slope of the regression line, and has no other significance.

Recommendation

Rather than use la_{MA20} or even la_{INT} , the slope of the regression line (n_{log}) may be used as the abrasion index. In this way five times more data is used in determining the index, i.e. all the penetrations from 1000 to 5000. The linearity of the lines plotted according to expression (9-12) suggests that this form of calculating abrasion wear is most accurate.

Low n_{log} values indicate low abrasion wear while high n_{log} values indicate high abrasion wear.

One disadvantage of using the n_{log} index, however, is that it requires a higher level of understanding and interpretation. Not all specifiers/manufacturers/contractors will be comfortable with it.

9.6.4 n_{vol} - an index based on the slope of the V versus P graph

A simple method of expressing abrasion was developed in 9.5.2, where it was shown that the volume of abraded material is nearly linear with respect to revolutions of the ball race. This is particularly so when the range between 1000 and 5000 revolutions is examined. The equation $V = n \times R$ (expression 9-9) was developed. As for the logarithmic expression in 9.6.3 (see figures 9.11, 9.12, 9.13), the n of expression 9-9 also represents the slope of the lines in graphs where V is plotted against R .

Appendices J.9 through J.16: The V values (volume of groove) for the 48 mixes are recorded here (calculated from the P values of appendices J.1 through J.8).

Appendices J.41 through J.48: For each mix a linear regression analysis tests the degree to which the V values (corresponding to R_{1000} , R_{2000} , R_{3000} , R_{4000} , and R_{5000}) are in a straight line. (Each V value is the average of 5 blocks). In order to demonstrate the linearity of the results the coordinates corresponding to mixes 1.1, 2.2, and 2.5 are plotted on figure 9.17, and the respective regression lines are shown.

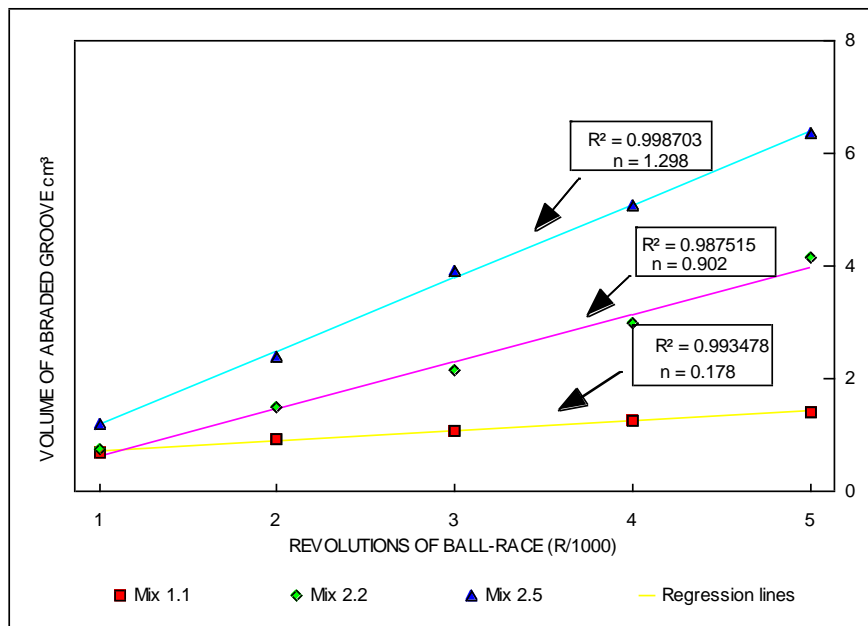


Figure 9.17 Relationship illustrating linearity between revolutions of race-way and volume of abraded groove. (Note that this applies to pavers that have been uniformly cured, and will likely not hold true where surface properties differ from the core's).

Comments

Figure 9.17 illustrates the relationship between abraded volume of the groove and revolutions for the same mixes illustrated in figures 9.14 through 9.16. The excellent linear correlation for the range P_{1000} through P_{5000} is apparent from this figure and from the near perfect R^2 values of the order of 0.99. It would therefore appear that expression 9-9 indicates near constant volume loss for the MA20 test. Once again, mix 1.1, which is known to have the lowest abrasion wear, has a much lower slope than mix 2.5 which is known to have a much higher abrasion wear, this suggesting that the slope of the V vs P graphs, n_{vol} , could be a useful alternative abrasion index. This may be expressed as:

$$\text{Abrasion-wear index} \propto n_{vol} \dots\dots (9-14)$$

9.6.5 P_{5000} - an index based on the abraded depth of the groove

The simplest possible way of expressing abrasion wear is to equate the abrasion index with the depth of the groove, i.e.:

$$P_{5000} = P = \text{Penetration at 5000 revolutions} \dots\dots\dots (9-15)$$

The various depths of penetration for all the MA20 abrasion testing are recorded in appendices J.1 through J.8.

If the penetration is only available for a lesser number of revolutions (e.g. see appendix J.3) then expression 9-16 below can be used to determine the equivalent penetration that would have occurred if it were possible to continue the test till 5000 revolutions:

$$P_{5000\text{equiv}} = \sqrt{5/\sqrt{R_{\text{actual}}}} \times P_{\text{actual}} \dots\dots\dots (9-16)$$

Expression (9-16) allows the abrasion wear of inferior surfaces to be compared with those that can go the full distance of 5000 revolutions and accordingly has been applied to appendices J.1 through J.8 where required. Thus a full set of P_{5000} results (including $P_{5000\text{equiv}}$ results) are recorded in column F of table 9-2.

Clearly equation (9-16) assumes penetration is directly proportional to the square root of the revolutions for all the mix designs, which is not always the case. It may be seen in column E of table 9.2 that the exponential may be as low as 0,266 or as high as 0,86, although the average value is seen to be 0,555, which is not very far from the assumed value of 0,5.

9.6.6 V_{5000} - an index based on the abraded volume of the groove

Having established the depth of penetration for a certain number of revolutions, expressions (9-4), (9-6) and (9-7) may now be used to calculate the volume, V , of the resulting groove. This has been done and the values V_{1000} , V_{2000} , V_{3000} , V_{4000} and V_{5000} are recorded in appendices J.9 through J.16. (Note that these appendices are in fact an extension of appendices J.1 through J.8, which record the relationship between depth of penetration and revolutions). The relationships between V and R for mix designs 1 through 8 are illustrated in appendices J.25 through J.32.

An alternative method of determining V_{5000} is to measure the volume of the groove after 5000 revolutions using plasticine, but with the aid of a computer the calculation method is a cleaner and quicker solution.

In this case the abrasion index, which expresses abrasion wear, may simply be stated as:

$$V_{5000} = V \text{ as determined from expressions 9-16, 9-4, 9-6, 7-6} \dots\dots\dots (9-17)$$

9.6.7 Critical evaluation of the abrasion indices

In the preceding sections, 9.6.1 through 9.6.6, six different indices were considered for the MA20 abrasion test, viz. I_{MA20} , I_{INT} , n_{log} , n_{vol} , P_{5000} , V_{5000} .

The question that must now be answered is 'Which is the best one?'

The primary requirement of any abrasion index is to accurately indicate either the abrasion-wear or abrasion resistance of the blocks. However, since the existing index, I_{MA20} , is being examined, it cannot therefore also be used as a yardstick for assessing other indices. Therefore in the absence of an abrasion test with proven, established and meaningful indices, the results of the parallel compression tests will be used as the benchmark for assessing the various abrasion indices. (It was explained earlier that compressive strength, in this investigation, can be considered as representative of abrasion resistance. In a recent investigation Shackel(1992)also found good correlation between abrasion resistance and compressive strength for concrete cubes made under carefully controlled laboratory conditions. Likewise section 2.1.5 of volume 2 cites many investigators who found this to be so, and where not the case, a suitable explanation could generally be found).

The general approach therefore will be to correlate the various abrasion indices against compressive strength. This is done for each of the indices in figures 9.18 through 9.23, and a best fit line is shown in each case, as well as the correlation coefficient, R^2 . *The index that has the lowest coefficient may thus be regarded as 'the best one'.*

In order to construct the various correlation graphs, Table 9.2 conveniently records the six abrasion indices alongside each other and alongside the compressive strength (see column B of table 9-2), for all of the 48 mixes. In each case the 'average' compressive strength of all three crushing tests was used (see discussion in chapter 7). This parameter represents the mean of 18 blocks, and is thus a very good indication of the quality of each of the 48 mixes.

MIX	AVERAGE MPa	la _{MA20} n=0.5	la _{INT} n=0.5	n _{log}	n _{vol}	P ₅₀₀₀ mm	V ₅₀₀₀ cm ³
A	B	C	D	E	F	G	H
1.1	38.5	2.182	2.055	0.317	0.178	1.09	1.39
1.2	39.5	2.300	2.214	0.409	0.195	1.01	1.25
1.3	32.6	1.674	1.604	0.478	0.344	1.39	2.00
1.4	23.1	0.986	0.958	0.530	0.757	2.33	4.25
1.5	23.6	0.908	0.882	0.564	0.888	2.53	4.78
1.6	18.1	0.699	0.686	0.587	1.298	3.26	6.89
2.1	30.7	0.992	0.924	0.633	0.902	2.42	4.49
2.2	31.3	0.927	0.908	0.533	0.831	2.46	4.59
2.3	29.3	0.959	0.900	0.576	0.873	2.48	4.65
2.4	23.0	0.670	0.666	0.628	1.389	3.36	7.19
2.5	20.4	0.737	0.727	0.728	1.298	3.08	6.35
2.6	18.1	0.678	0.655	0.482	1.805	3.41	7.35
3.1	20.9	0.735	0.635	0.536	1.580	3.52	7.70
3.2	19.1	0.554	0.525	0.860	2.675	4.26	10.06
3.3	16.1	0.502	0.512	0.800	2.925	4.38	10.46
3.4	13.7	0.395	0.371			6.04	16.27
3.5	12.5	0.343	0.297			7.54	21.78
3.6	13.4	0.376	0.373			5.99	16.10
4.1	27.9	0.835	0.797	0.796	1.168	2.81	5.57
4.2	29.1	0.856	0.835	0.571	0.953	2.68	5.20
4.3	17.4	0.475	0.481			4.65	11.36
4.4	16.1	0.430	0.423	0.671	3.040	5.29	13.60
4.5	17.0	0.462	0.459			4.87	12.14
4.6	15.7	0.424	0.477			4.70	11.53
5.1	32.3	1.284	1.231	0.460	0.495	1.82	2.96
5.2	26.6	1.280	1.249	0.395	0.443	1.79	2.89
5.3	20.7	1.042	0.928	0.725	0.964	2.41	4.46
5.4	21.5	0.928	0.846	0.612	0.993	2.64	5.09
5.5	18.8	0.536	0.562	0.590	1.950	3.98	9.13
5.6	14.1	0.390	0.407			5.50	14.33
6.1	31.2	0.947	0.923	0.452	0.739	2.47	4.62
6.2	29.4	0.887	0.870	0.666	0.968	2.57	4.89
6.3	23.2	0.767	0.770	0.655	1.172	2.91	5.85
6.4	19.4	0.554	0.557	0.675	2.125	4.01	9.26
6.5	16.7	0.443	0.460			4.85	12.07
6.6	13.4	0.368	0.360			6.22	16.91
7.1	35.7	1.499	1.444	0.266	0.296	1.55	2.34
7.2	31.7	1.549	1.489	0.383	0.334	1.50	2.23
7.3	25.6	0.977	0.961	0.591	0.787	2.33	4.25
7.4	24.8	1.198	0.967	0.511	0.757	2.31	4.19
7.5	20.9	0.772	0.856	0.587	1.255	2.61	5.00
7.6	16.9	0.482	0.476			4.70	11.53
8.1	33.8	1.603	1.475	0.344	0.326	1.52	2.28
8.2	35.0	1.797	1.786	0.442	0.276	1.25	1.71
8.3	35.5	1.734	1.606	0.352	0.283	1.39	2.00
8.4	23.9	1.257	1.071	0.529	0.691	2.09	3.63
8.5	22.3	0.995	0.942	0.507	0.770	2.38	4.38
8.6	20.3	0.684	0.696	0.654	1.419	3.22	6.77
Average	23.8	0.918	0.881	0.555	1.056	3.20	7.08
No. of mixes	48	48	48	38	38	48	48

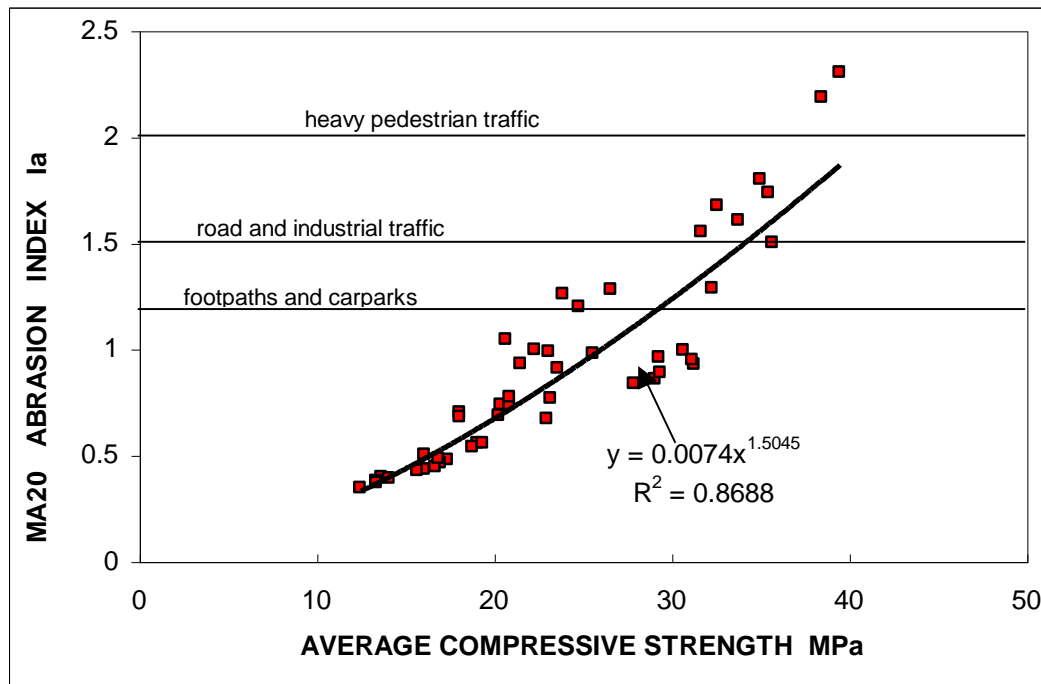


Figure 9.18 Relationship between MA20 abrasion index, $I_{a_{MA20}}$, and average compressive strength. The three interim abrasion limits are shown at 1.2, 1.5, 2.0.

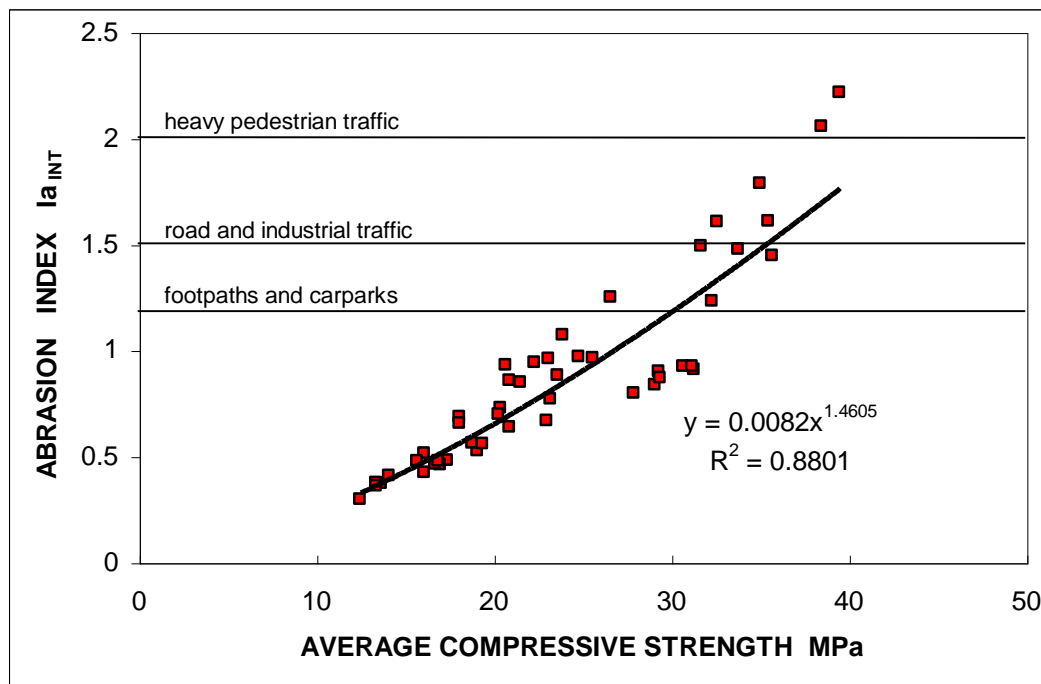


Figure 9.19 Relationship between abrasion index $I_{a_{INT}}$ and average compressive strength.

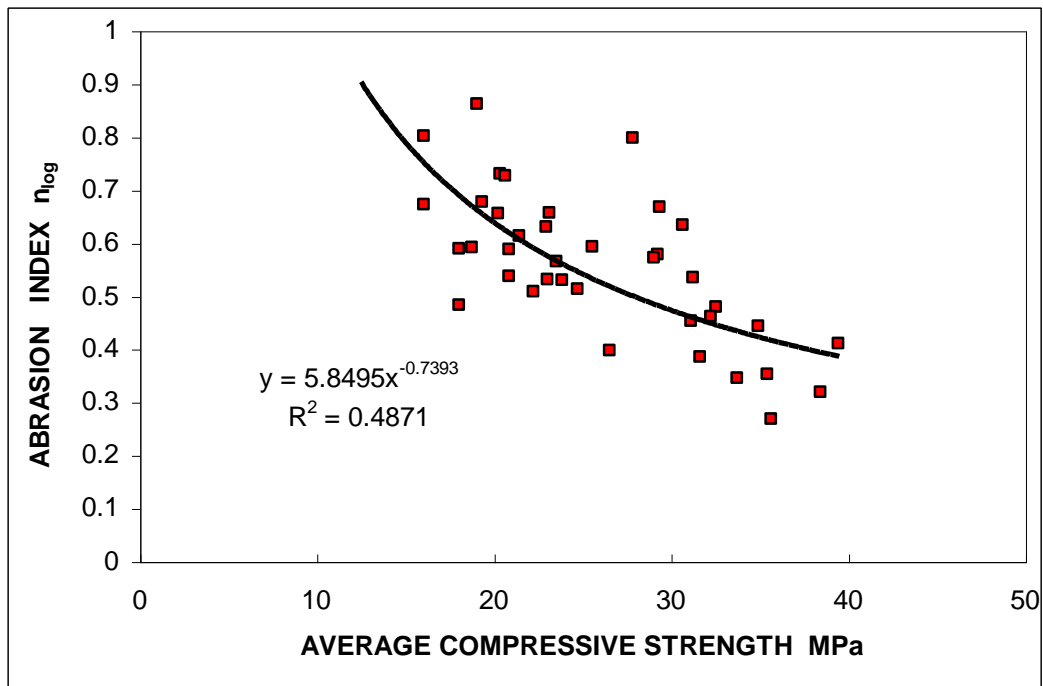


Figure 9.20 Relationship between abrasion index n_{log} and average compressive strength

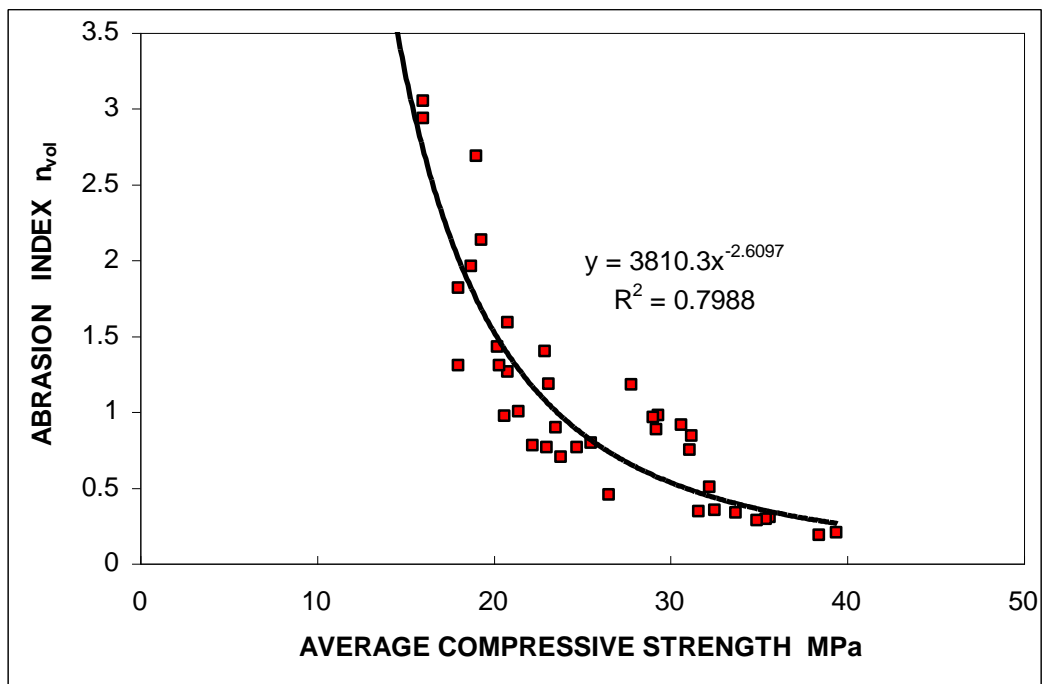


Figure 9.21 Relationship between abrasion index n_{vol} and average compressive strength

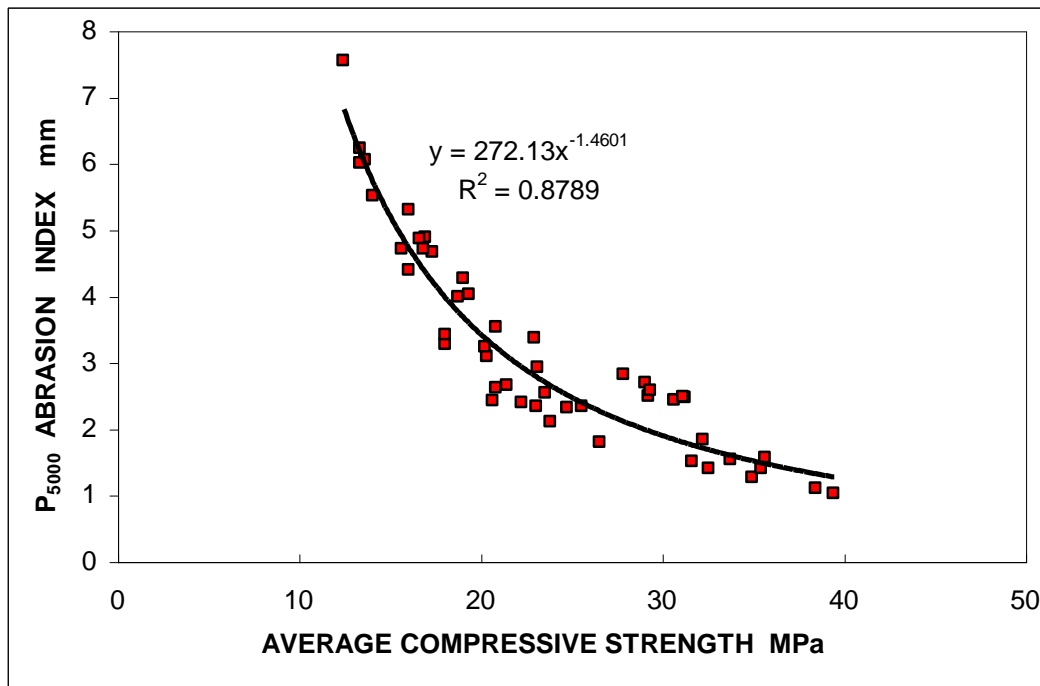


Figure 9.22 Relationship between abrasion index P_{5000} and average compressive strength

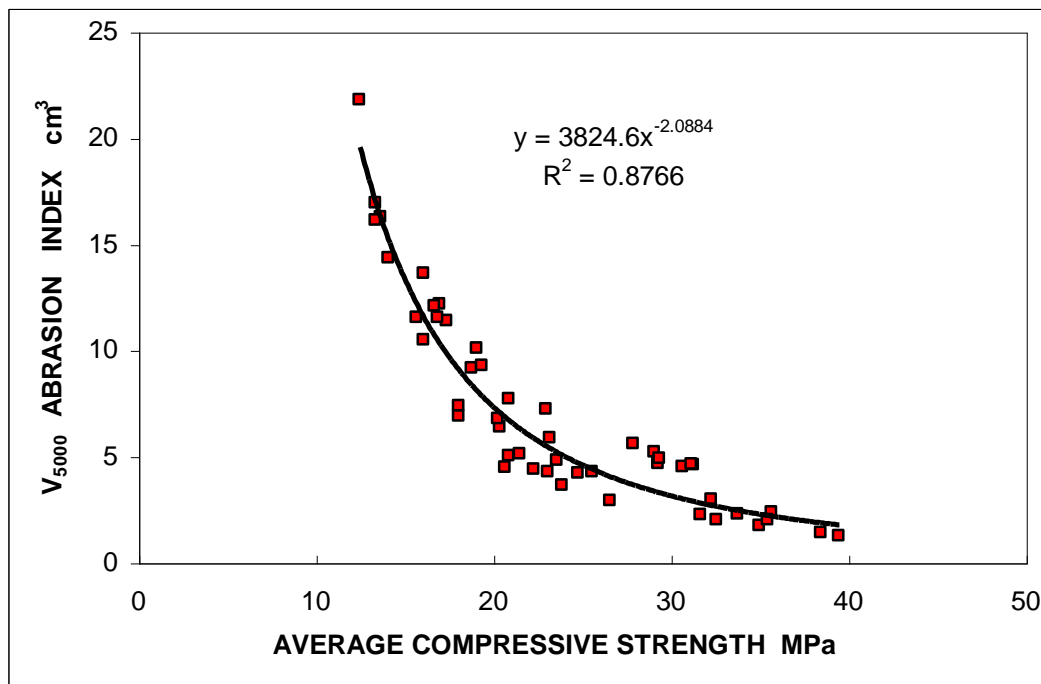


Figure 9.23 Relationship between abrasion index V_{5000} and average compressive strength

Observations and Discussion

1. Coefficients of Variation

The coefficients of variation indicating the degree of correlation between the abrasion indices and compressive strength in figures 9.18 through 9.23 are shown in table 9-3. It is evident that there is a good correlation for four of the indices, i.e. $I_{a_{MA20}}$, $I_{a_{INT}}$, P_{5000} and V_{5000} , and that there is very little to choose between them.

The closeness of the correlation coefficients for the first two coefficients is expected, as both of them are a function of the reciprocal of P , and the slight difference is explained by the difference in their respective formulae (see expression 9-10 and 9-11). The use of the $I_{a_{INT}}$ index in this investigation rather than official $I_{a_{MA20}}$ is therefore of no consequence.

The closeness of the correlation coefficients for the first two coefficients relative to the last two in table 9-3 is perhaps unexpected, given that the former two are a function of the reciprocal of P , while the latter two are directly proportional to P . The explanation is that the 'best fit' curves in each of the figures are power functions, and it may be shown that the correlation coefficient for a power/exponential trendline of a set of coordinates is the same as that for a power/exponential trendline of the reciprocal of those coordinates.

It follows that the closeness of the correlation coefficients for the above stated indices means that any one of them can successfully simulate the quality of the concrete in this investigation, and therefore any one of them may be chosen.

On the other hand, while the regression lines for n_{log} have excellent R^2 values on a mix by mix basis (see appendices J.33 through J.48), indicating very good alignment between the $\log P$ and $\log R$ coordinates *for a given mix*, a linear regression line through all the n_{log} values (see figure 9-20) indicates relatively poor correlation with compressive strength ($R^2 = 0,487$). This implies that the slopes of the $\log P$: $\log R$ wear-duration curves are not strongly related to compressive strength and by extension abrasion wear.

The correlation of n_{vol} with compressive strength ($R^2 = 0,799$) is much better than that for n_{log} , but not as good as the other four.

Type of Abrasion Index	Correlation coefficient
$I_{a_{MA20}}$.8688
$I_{a_{INT}}$.8801
n_{log}	.4871
n_{vol}	.7988
P_{5000}	.8789
V_{5000}	.8766

2. MA20 'Interim' Limits

Figure 9.18 and 9.19 have three horizontal lines representing the three abrasion 'interim' limits in MA20. Considering figure 9.18 firstly, it appears that only two results of this investigation are suitable for 'heavily trafficked pedestrian pavements' (limit = 2,0), and only six could be used for 'public roads, industrial hardstands' (limit = 1,5), and only a further four could be used for 'lightly trafficked areas' (limit= 1,2). The other 36 mixes would fail. This situation is even worse in figure 9.19.

However, the actual wear measurements at Westgate after 6 years (see chapter 14) indicate that these limits are too severe, and that a number of mixes that are below the

bottom line (limit = 1,2) performed acceptably. The following explanations are offered for the lower than expected 28-day indices:

- (1) the official 'interim' MA20 indices are based on testing the blocks in a dry state, whereas they were soaked for 24 hours in these tests. Sukandar(1993), who did testing with the similar ASTM C779 Proc C test, concluded that abrasion resistance was far more sensitive to moisture conditioning than compression testing and found a reduction in abrasion resistance of up to 111% for blocks tested wet, although this percentage reduced to 15% for the strongest blocks. This tendency alone is enough to render the MA20 limits virtually meaningless in this investigation.
- (2) one of the eight mix designs, No 3, was purposely made with a low binder content
- (3) at least half of all the mixes were made with too little water
- (4) three of the eight mixes incorporated fly ash and were noticeably retarded in their 28 day strength development relative to the control

Sectional Conclusion

A strong effort has been made in this section to find an alternative means of expressing the MA20 abrasion index, in the hope of finding an index with a high correlation coefficient relative to compression testing. Four of the six indices all had correlation coefficients, of approximately 0,87. This allows the use of la_{INT} in this investigation as a substitute for official la_{MA20} , while at the same time sanctioning the use of direct *depth of penetration* or *volume of groove* as alternative indices. Notwithstanding, the la_{INT} index will generally be retained in the balance of this document where the MA20 test is concerned. It has both the highest correlation coefficient (0,88) and is closely related to the well known la_{MA20} index.

9.7 The Variability of the MA20 Test

In the previous section it was shown that a relatively strong correlation exists between compressive strength and the la_{INT} abrasion index ($R^2 = 0,88$), indicating that this index is a useful indicator of quality. In determining this correlation, the *48 abrasion indices* were compared to 48 compressive strengths, where the former indices were each the average of 5 tests, each on a different paver, and the latter strengths were each the average of six blocks crushed.

While the correlation coefficient of section 9.6 gives useful information regarding the distribution of the 48 indices, and it bears repeating that each of these indices is the mean of five abrasion tests, it does not indicate the variation/scatter within the five individual indices. Such aspects as the range, the minimum and the maximum, the standard deviation, and the coefficient of variation, are not incorporated into the correlation coefficient of section 9.6, which only makes use of the mean.

In order for a test to have a good repeatability, it is important that the individual results do not deviate significantly around the mean, i.e. they should have a low coefficient of variation.

The repeatability of the MA20SA test is not as good as that of the wirebrush and sandblast tests, with the respective average of 48 coefficients of variation (5 samples per mix) measuring 24.3%, 15,1% and 7,7% (from table 12.4). This should also be seen in the light of the average of 48 coefficients (6 samples per mix) for the three compression tests, respectively, 10,4 % for the SABS test, 9,2 % for the ASTM C140 test, and 8,7 % for the MA20 test.

Shackel(1992), in a critical evaluation of MA20, found a number of factors that contribute to the variability of the test. Some of these findings offer an explanation for the relatively high average coefficient of 24,3 % in this investigation, discussed in 9.7.1 through 9.7.4:

9.7.1 Mean of five samples

Shackel found that the mean of five abrasion values (used in their work) is inadequate to delineate the abrasion resistance, since in this case la varies by $\pm 0,45$ at a confidence level of 95%. Increasing the test samples to ten is beneficial to the precision of the test, and in this case la varies by $\pm 0,31$ at the 95% confidence level.

9.7.2 Misalignment

Misalignment as small as $0,5^\circ$ between the specimen and the drill chuck can significantly influence the results. Misalignment of 1° can influence the abrasion index by as much as 35%. The authors state that misalignments of 1° are unlikely in practice, even difficult to achieve. [The writer is not in agreement here; he has seen a number of tests where the width of the eventual groove is noticeably narrower on one side, and the misalignment appears to be more than 1° . Misalignment was a definite possibility with the blocks used in this writer's investigation, which had somewhat uneven undersides owing to the imprint of the wooden pallets. This could therefore have contributed to the high coefficient of variation].

9.7.3 Worn bearings

The balls used in their tests show a slight decrease both in ball diameter and Rockwell C hardness with use. The test data suggest that the balls should be replaced once they have served in about 65,000 ball-race revolutions.

Their work shows a significant increase in I_a of approximately 1,0 after 65000 revolutions.

The implication here is that the steel balls were no longer significantly harder than the concrete surface. According to Hutchings(1992), the concrete will be abraded only if the hardness of the abrasion medium exceeds 1,2 that of the concrete surface.

Table 9-4, reproduced from Hutchings(1992) shows that quartz has an indentation hardness that typically varies between 750 and 1200, and this may be taken as the hardness of the concrete surface in this investigation, given that the aggregate was reef quartzite. By way of contrast it may be seen that most steel alloys either have a hardness that is in the same range or less. Therefore if through vibration and gradual attrition the balls loose some of their hardness, and this hardness is no longer greater than 1,2 that of the concrete, then it seems plausible that abrasion in the concrete will be slower.

Table 9 – 4 Hardness values for common abrasive particles and phases or constituents of steels and cast irons	
	Material Hardness (HV)
1. Typical abrasive materials	
Diamond	600-10000
Boron carbide, B_4C	2700-3700
Silicon carbide	2100-2600
Alumina (corundum)	1800-2000
Quartz (silica)	750-1200
Garnet	600-1000
Magnetite Fe_3O_4	370-600
Soda-lime glass	~ 500
Fluorite, CaF_2	180-190
2. Phases or constituents of steels and cast irons	
Ferrite, α -Fe	70-200
Pearlite (plain C)	250-320
Pearlite (alloyed)	300-460
Austenite (12% Mn)	170-230
Austenite (low alloy)	250-350
Austenite (high Cr)	300-600
Martensite	500-1000
Cementite, Fe_3C	840-1100
Chromium/iron carbide, $(Fe,Cr)_7C_3$	1200-1600

On the other hand it is also possible that this apparent increase in hardness may have been a result of wear in the brass housing used to locate the balls, rather than the 'slight' decrease in the hardness of the balls themselves. Any wear in the brass housing would allow the balls to wobble around in their orbit, resulting in the formation of a wider groove, at the expense of depth of penetration. The reduced depth would naturally register as an increase in I_a . Note that a wide groove in the MA20 is further made possible by a relatively poor lateral guide system.

In support of this supposition the steel cage of the bearing used in the writer's investigation showed an increase in the size of the holes, and this would similarly lead to an increased *la*. The interval between bearing changes was generally in excess of 65,000 revolutions, and thus the transition from new to used would account for some variability in results.

9.7.4 Secondary factors

Shackel(1992) found that the weight of the drill, the rate of water flow, the ball race speed, and the bedding in period have only a small influence on the overall test variability.

Many of the recommendations reported in 9.7.1 through 9.7.4 have been adopted into the proposed CMA20 specification (see appendix A.6) in order to reduce variability.

9.7.5 Discussion

By incorporating these 1992 improvements into the MA20 test, Shackel(1993b) obtained coefficients of variation ranging between 11,54% and 11,79%, on tests done on the sides of carefully prepared concrete cubes. This appears to be superior to the 17,74% variability that the ASTM C779 test claims for itself, but it is not known how ASTM derived this. What is known, is that Sukandar(1993), using the ASTM test in a study on eight sets of factory made *concrete pavers*, obtained coefficients of variation ranging from 6,7% to 17,3%, with an overall average of 9,5%. This is even less than Shackel results. That Sukandar's average variability for factory made pavers was lower is seen to be significant, since it goes against the expected trend which dictates that the *sides of laboratory made cubes* should invariably have a lower variability than the *surface of factory made pavers*. The implication here is that the ASTM C779 test (or at least Sukandar's version of it – he used a core testing machine as the driving unit) in fact has a lower variability than the MA20 derivative. This seems to indicate that the MA20 test equipment is not as good. Both the drill and the drill-stand in Sukandar's work appear to be significantly sturdier than the MA20 hand-drill mounted in a drill stand. This means that vibration, bouncing and impact would be less, and there would also be a lesser possibility for lateral movement.

Interestingly the MA20 coefficient of variation of 11,5% as determined by Shackel(1993a) is about 2,3 times more than what might be expected in the variability of crushed concrete cubes (a C.of V.of 5% would be typical for carefully made cubes). If this same factor is applied to the findings of this investigation, then a C. of V. of 23.2% / 2,3 = 10% could be expected for the crushing tests. These values do indeed seem to tie in with the compression tests of this investigation; SABS 1058 variability was 10,4% while that of ASTM C140 was 9,2%. On the other hand Sukandar(1993)'s ASTM C779 variability was only 30% more than his ASTM C140 compressive strength.

In conclusion the following deductions may be made:

- (1) The ball-bearing test has a greater variability relative to the compressive strength test:
 - The ASTM C779 test seems to be more variable than the ASTM C140 compression test by a factor of 1,3 (Sukandar).
 - The MA20 test (on pavers) seems to be more variable than the SABS and ASTM compression tests by a factor of 2,3. This same ratio appears to apply to cubes, although cubes have a substantially lower variability.
- (2) ASTM C779 seems to have a lower variability than MA20, in spite of ASTM claiming the relatively high variability of 17,74%. (Compare Sukandar's 9,5% with Shakel's 11,5%).

- (3) Cubes tested on their sides have lower variability compared with pavers tested on their tops (Compare Shackel's 11,5% with the 24,3% of this investigation). However, it is not known to what extent this difference may be attributed to the improvements made to the test method in 1992. It is possible that by including the findings and recommendations of Shakel(1992) similar figures can be achieved for CMA20 (the proposed modified test method recommended to the CMA in 1994).

Recommendation: Parallel testing should be done on MA20 and ASTM C779, to establish more precisely their relative variabilities. If the stigma of poor variability can be eliminated, the MA20 test would be a most suitable abrasion test.

9.8 Limiting Criteria

The interim criteria set in 1986 for the MA20 test (see 9.3) were never formally adopted, but were nevertheless in widespread use in Australia. Following further investigations Shackel(1992) warned that 'tests on pavers extracted from several block pavements indicate that values of Ia below 1,0 are generally associated with unsatisfactory wear performance. However it has not yet proved possible to verify the abrasion performance limits'.

One of the stated objectives of this research is to establish such limiting criteria from the measured wear of trafficked blocks at the Westgate site (see chapter 15).

9.9 MA20SA specification

The MA20 test in this investigation differs in some ways from the MA20 test in Australia. This came about partly by accident and partly by design, the former as a result of not appreciating some of the finer points in the test method. These points are discussed below.

9.9.1 Soaking

The Australian specification calls for blocks to be tested dry, whereas in this research and other research done locally [Holland(1991), Robertson(1991)] the blocks were tested after being soaked in water for 24 hours. In South Africa the standard method of preparing blocks or cubes for compression testing is to soak the specimens for 24 hours, which has the effect of ensuring that all tests are done at the same moisture condition, and it was logical to assume that this would also be the case for abrasion resistance testing.

However, Shackel(1985) reports that an advantage of testing dry is a reduced standard deviation. He also found, as may be expected, that dry testing resulted in less wear on the blocks. This is confirmed by Ghafoori(1992) who found that blocks tested dry with the ASTM C779 apparatus (similar to MA20) had on average an increased abrasion resistance of 49%, compared to the equivalent soaked blocks. The precise ratio varied from 15% for very rich mixes (33% binder), to as much as 108% for lean mixes (11% binder).

The significant effect of moisture content highlights the importance of achieving a consistent moisture conditioning, and since it is difficult to define how dry 'dry' is, it is more practical to soak the pavers.

9.9.2 Number of balls

A further point of departure is that MA20 calls for a ball-race with 12 balls as opposed to 13 balls as used in this research. (The bearing with 12 balls is not a stock item in South Africa, and there would be no point in expecting paving manufactures to start importing when a very similar bearing is locally available at a lower cost). The effect of having an extra ball is that the compressive stress exerted on the concrete will be reduced by a factor of 12/13 (the diameter of the balls are the same in both cases). However the number of ball passes at any given point will be increased by a factor of 13/12. These two factors may cancel each other, and hence the rate of wear may be the same in the end.

The difference in the balls between the three tests is summarised in table 9.A below:

	ASTM C779	MA20 CMAA	MA20 SA
Number of balls	8	12	13
Diameter of balls (mm)	18.25	15.83	15.83
Compressive force (N)	120	160	167
Speed in revs/minute	1000	1000	1000

9.9.3 Construction of Bearing

A significant difference exists in the bearing. In the Australian test the 12 balls are located in a heavy brass ball locating ring such that only six balls protrude on either side. This means that six balls are in contact with the thrust cup (race-way) on the upper side of the ring, while the six below the ring make contact with the paver.

In the bearing used in South Africa, the locating ring consists of a relatively thin circular steel plate that has been formed such that the bearings will not fall out (see figure 4.12). Most significantly however, all 13 balls in the SA test protrude equally on both sides of the locating ring, and therefore all 13 balls make contact with both the race-way and the block at the same time.

Thus in the South African test, there is virtually no drag effect on the balls as they are made to roll on the surface of the block under load, but in the Australian test the balls are not free to rotate; there is some drag from the brass ring. The resultant friction is the product of the mass of the drill and the coefficient of friction of steel-on-water-lubricated-brass.

It may therefore be postulated that the rate of abrasion wear will be greater in the case of the Australian test, given that there will be some frictional/sliding effects in addition to normal crushing, but the magnitude and effect of such frictional resistance is yet to be established.

It is also apparent that since MA20 has only six balls in contact with the concrete relative to the 13 of MA20SA the compressive stresses will be greater by a factor of 13/6. Alternatively the same effect would be achieved in MA20SA if the load were increased by the same factor. The affect of an increase in load is considered in the next section.

9.9.4 Heavier apparatus

The MA20SA test drill and sliding bracket has a mass of 17 kg, while in the Australian test it is 16 kg. According to Shackel(1992), the effect of increasing the mass from 16kg to 20kg has a 'negligible' effect on the abrasion index. A possible explanation is that at both 16kg and 20kg the stress on a macro-scale was within the concrete's elastic range, and thus no crushing would take place (macro-scale). A consideration of figure 9.9 shows that the stress beneath the balls, on a macro-scale, and assuming a purely static load, quickly reduces to less than 3 MPa. This however applies to the MA20SA bearing, which means that it would be of the order of 6MPa for the MA20 bearing. But even assuming 6MPa and a further 25% additional weight (20kg rather than 16kg), it is clear that the macro-scale stress would still be well within the elastic strength range of most concretes.

Yet it is plain that abrasion wear continues with increasing revolutions at a virtually constant rate (see figure 9-11). This supports the supposition that crushing takes place at the microscopic asperities where stresses are highly magnified. Therefore since microscopic crushing continues with ongoing revolutions for the case of a constant load, it is logical that

as the load increases the degree of microscopic crushing will increase proportionately. So while Shackel(1992)'s finding can be explained by arguing that on a macroscopic scale compressive stresses remain in the elastic zone as the load increases from 16kg to 20kg, considerations of microscopic crushing argue against these findings.

9.9.5 Better guide system

The slightly larger mass of the SA test is partly attributable to the sliding apparatus, which has a greatly improved guiding system, shown in figures 4.13 and 4.14. This prevents sideways wander (lateral displacement) of the race-way.

9.9.6 Different fastening system

The method of fastening the block is also illustrated in figures 4.13 and 4.14, and can be seen to differ from the MA20 method, where the block is fastened from the side. However if the base of the block is not parallel to the surface, then in both of these methods it is possible to have the surface of the block at some inclination to a plane normal to the axis of the drill, and this has been shown to significantly effect the results [Shackel(1992)].

9.9.7 Depth of penetration

In the MA20SA test the test carries on until the locating ring is in danger of fouling with the surface of the block, whereas the Australian test is terminated after 1,5 mm of penetration. (Apart from this both tests run for five minutes).

9.9.8 Hardness of bearings

In this investigation the bearings were used beyond the 65000 revolution mark, and this has been shown to make a significant difference to the results [Shackel(1992)]. This may therefore contribute to the high coefficient of variation of 24,3%. See 9.7.3 for a fuller discussion on the effects of hardness.

9.9.9 CMA20 Tests

The CMA20 test is a further development of the MA20/MA20SA test. It addresses a number of factors that have been shown to result in high variability [Shackel(1992)]. For example, it has a method of fastening the block such that there is no misalignment of the bearing relative to upper surface of the block; there is an improved guide system; the test duration is only 2000 revolutions etc. This test is described in detail in appendix A.6. In 1993 the CMA members were considering routine testing with such an apparatus with a view to verifying its claims and possibly adopting the test as an industry standard. However the project was shelved after the high variability of MA20 caused concern in Australia.

9.10 Strengths and Weaknesses of MA20 Abrasion Test

In spite of the high variability of MA20, this test is still worth considering for testing paving blocks. It was chosen only after some 32 other tests, variously used around the world, had been considered [Rourke(1986)]. In 1986 it met all the requirements thought to be important by the CMAA (see introduction) for an abrasion test. It is a derivative of a test that is widely used in America, ASTM C779 Proc C. Some of these advantages are as follows:

9.10.1 Fast

It is fast enough to allow it to be used as a method of production control. The test takes about 7 minutes, including the time taken to fasten and correctly align the specimen and remove it afterwards.

If the test is terminated after 2000 revolutions, then this time will be reduced to four minutes. Shackel(1992) found that there was a strong correlation between 2000 and 5000 revolutions.

9.10.2 Severe

The severity of this test is attributable to the small contact area between the spherical balls and the surface at the beginning. At the start of the test the compressive stress beneath each individual ball is so high that the balls abrade even the strongest of concrete surfaces. For example, if it assumed that the combined contact area of 13 balls is 1mm^2 at the start of the test, and that the apparatus weighs 17 kg, then the compressive stress will equate to 167 MPa. It stands to reason that after 65000 balls (5000 revolutions of shaft x 13 balls) have passed over any given point in the track, even concrete with a compressive strength in excess of 100 MPa will fatigue to show a clearly defined groove. This was demonstrated by Horiguchi(1994) who achieved a penetration of 1mm using the ASTM C779 test on 116 MPa concrete.

The severity of the test in the initial stages therefore sets this test apart from other abrasion tests such as the ASTM C944 test, where a rotating cutter with a considerably larger bearing area (by virtue of many teeth in contact with the surface) is not as capable of producing a distinct penetration on high strength surfaces [Horiguchi(1994), see figure 5]. The wirebrush test makes even less of an impression. In concretes above 50MPa the bristles barely scratch the surface.

9.10.3 Surface test

In spite of the test being very severe in the initial stages, the shape of the wear-duration curve starts to level off somewhere between 500 and 1000 revolutions. (The ball:concrete contact surface area becomes greater, and hence the stresses beneath the balls are reduced). The test is not meant to continue below depths of 1,5 mm (except for very inferior blocks), and can therefore be regarded as a true surface test, unlike the ASTM C418 test that may penetrate as far down as 10 mm or more at the deepest part of the crater.

Using 2000 revolutions in the calculation of the abrasion index I_a , makes the test an even better measure of the quality of the surface skin, providing that it can be shown that a good

correlation exists for the indices corresponding to 2000 and 5000 revolutions.

Shackel(1992) found a 'strong' correlation between la_{P2000} and la_{P5000} on tests made on concrete cubes.

In this investigation, a relatively strong correlation has also been established for abrasion indices calculated respectively for 2000 and 5000 revolutions, i.e. $la_{INT} = 0.9222$, see figure 9-24. These indices were calculated from data in appendices J.1 through J.8 using the 'mean' penetrations at 2000 and 5000 revolutions for 28 of the mixes. The remaining 20 mixes could not be included as these tests had been stopped before 5000 revolutions.

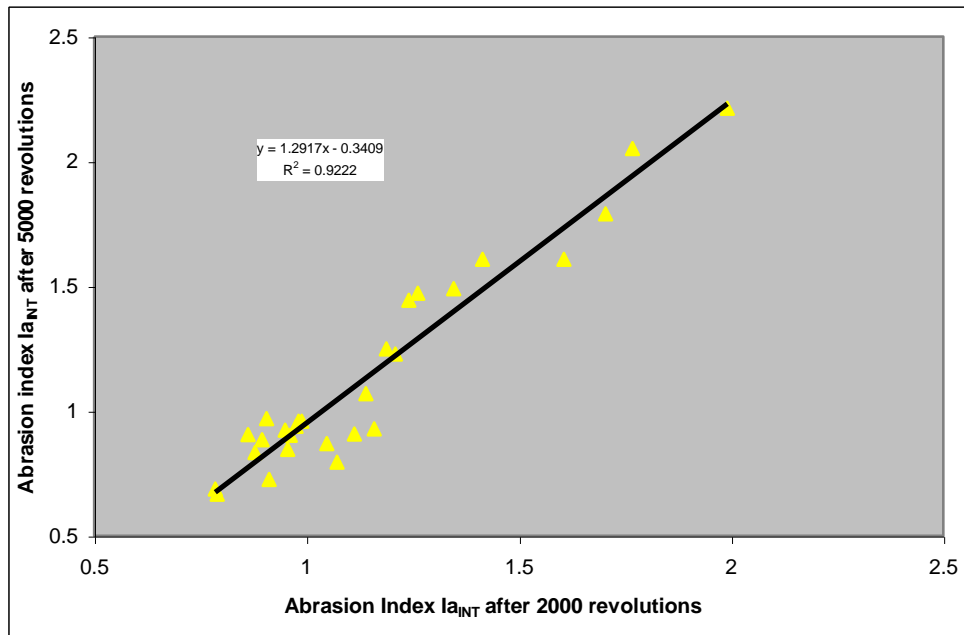


Figure 9.24 Correlation between la_{INT} at 5000 revolutions and la_{INT} at 2000 revolutions.

9.10.4 Capital expenditure

It is carried out with relatively inexpensive equipment. In 1994 the cost of this equipment, including drill, stand, optical rev counter, special chuck, clamp etc. was approximately R6000.00. (The improvements of the 'CMA20' test may however double this cost).

9.10.5 Portable

The equipment is portable and can easily be adapted to in-situ testing, by removing the clamping device and using a special base plate with a hole in the vicinity of the race-way.

9.10.6 Similar to existing tests

The South Africa version of MA20 has been modified, as discussed in 9.9 and is therefore referred to as the MA20SA test. Further modifications have been suggested (i.e. CMA20) in the light of Shackel(1992)'s findings.

Its similarity with ASTM C779 Proc C means that comparisons can be made with results done in the USA. In Australia, several investigators have published their findings on MA20, including their experimental results, allowing comparisons here too.

Recommendation: Tests should be made on carefully made concrete cubes, where one side of each cube may be tested with each of the four abrasion tests mentioned, i.e. ASTM C779 Proc C, MA20, MA20SA, and CMA20. If say 20 cubes can be tested in this way, an accurate assessment can be made of the net effect of the various differences. The different coefficients of variations will be of special interest.

9.10.7 Economic

It is relatively inexpensive on a test by test basis. The balls are exceptionally hard and can be used again and again without showing any appreciable signs of wear. The author found that the limiting factor was enlargement of the holes in the locating ring rather than wear in the balls, and that when a new bearing was used after approximately every 60 tests the balls had worn less than 0,1 mm. The cost of this bearing in 1994 was R180.00 and the cost per test was therefore R3.00.

Notwithstanding the minimal wear on the balls Shackel(1992) recommended that the bearing be changed after every 13 tests i.e. every 65,000 revolutions. This would increase the cost of each test to R13.85.

On the other hand, the relatively strong correlation between Ia at 5000 and 2000 revolutions, suggests it may be possible to take readings every 500 revolutions and stop the test at 2000. This would reduce the cost of each test to R5.54. This is a significant consideration, as most manufacturers would be reluctant to spend a lot of money on abrasion testing.

9.10.8 Reproducibility

Unless careful attention is applied to such aspects as:

- the inclination of the test specimen relative to the bearing,
- wear in the balls and locating ring,
- averaging at least ten tests for a result,
- ensuring adequate restraint against sideways wander of the drill

the test is unlikely to result in reproducible results from one laboratory to the next.

On the other hand, where the correct controls are in place, coefficients of variation as low as 12% are possible [Shackel(1992)].

9.10.9 Sensitivity

The MA20 test is the most sensitive of the three abrasion tests. This is shown globally by table 6.15, for all the mix designs used in this investigation, whereby the ratio of abrasion resistance for wettest mixes relative to driest is 2.5 for MA20, 1.63 for wire-clay and 1.54 for ASTM C418.

Still considering Table 6.15 the equivalent ratio for wettest compressive strength to driest is 1.85, indicating that MA20(abrasion) is more sensitive to mix design variations than compression testing. Moreover, Ghafoori(1992) found that whereas compression testing registered a 100% change due to changes to his mix designs, the ASTM C779 Proc C test (similar to MA20) registered a change in the order of 300 %.

A look at figures 9.4 through 9.6 shows that at 3000 revolutions, the depth of abrasion for the 2nd highest moisture content corresponding respectively to 10%, 14% and 18% binder,

was 3.3 mm, 1.6 mm and 0,8 mm.

These results reveal another feature of MA20; the rate of abrasion increases exponentially as the mix becomes weaker. This tendency is much more noticeable in MA20 compared to the other two tests (see figure 12.7). This may be explained as follows: the MA20 test applies a substantially greater force upon individual aggregate particles relative to the wirebrush and sandblast tests. The full mass of the drill is distributed over 13 steel balls (MA20SA), whereas the load on the wirebrush is distributed over *hundreds of flexible* wire bristles, while in the case of the sandblast test the load due to an individual grain of impacting sand is relatively small. The greater force on individual aggregate particles in the case of MA20 results in the aggregate/paste bond being broken if the paste lacks bonding ability. This may occur without the paste being abraded away around the particle and it leads to aggregate dislodgement rather than aggregate abrasion. Thus the departure from a straight line in the MA20 abrasion-wear expression represents aggregate loss by dislodgement rather than by microscopic crushing processes. Clearly the amount of aggregate lost will be related to the aggregate/paste bond and this is related to the cement content. These effects are further evidenced in the acceleration in abrasion that occurs from figure 9.4 (18% binder) through figure 9.5 (14% binder) through 9.6 (10% binder). It may therefore be said that the contribution of the aggregate in MA20, while very significant at 18% and 14% mixes, is undermined in mixes of 10%, and particularly where the mix was too 'dry'.

Although the sandblast and wirebrush processes also displace aggregate before it has abraded away, this occurs only after a substantial amount of paste has been abraded. Therefore in these tests it is the hardness of the paste that governs the wear processes. The absence of an acceleration in the wear process in figure 12.7 as cement contents are decreased seems to indicate that paste quality largely determines the rate of abrasion.

Summarising: The exponential increase in abrasion wear in the MA20 test with declining binder content indicates its greater sensitivity relative to the other tests. By virtue of its bond breaking and dislodgement capabilities, it is particularly sensitive to weak mixes.

9.10.10 Aggregate component

The characteristic appearance of the abraded surface in plan is that of a circular groove of diameter 75.1 mm, and in cross section that of a segment of a circle with diameter approximating that of the balls, i.e. 15.8 mm. A visual examination of the surface texture of the groove reveals a smooth evenly abraded surface (although there may be some evidence of waviness). There is no obvious protrusion of aggregate particles relative to the mortar component or vice versa, unlike the ASTM C418 and Wirebrush tests. This means that the MA20 test measures the combined strength of the aggregate and binder. The even penetration of the ball-race into the surface means that a hard aggregate will protect a weak binder, as would a strong binder protect a weak aggregate.

However, where the paver was made with a weak paste, there is clear evidence of small holes in the wear path where small aggregate particles had been debonded and washed out. This leads to an acceleration in abrasion as discussed in 9.10.9.

In most applications where cbp is used, surfaces wear in such a manner that the binder paste / mortar component abrades until the uppermost aggregate particles are exposed. From this point on the aggregate offers a measure of protection to the binder paste / mortar. Thus the aggregate plays a major part in the abrasion resistance of cbp surfaces. This is a major advantage of the MA20 test. The ASTM C418 and wirebrush tests do not similarly measure the contribution of the aggregate.

9.11 Summary, Conclusion, and Recommendation

The origins of the MA20 abrasion test date back to the ASTM C779 - 82 test. In 1986, after some modifications, it became the official test method of the Concrete Masonry Association of Australia, although the limits never progressed beyond the status of 'interim'.

The mechanism of the abrasive wear is essentially micro crushing; the protruding microscopic peaks of the concrete surface are crushed by the steel balls. This is a greatly accelerated simulation of what happens on most cbp surfaces, especially considering that the abrading medium in most applications is much softer; a rubber tyre or a leather sole.

Over and above the micro-crushing effects, there are also some secondary shear elements, from 'Heathcote slip', as well as some impact effects from vibration and bouncing. Accordingly this test is graded in table 4.2 of volume 2 as 'R3S1I2' to respectively indicate the relative contributions of rolling, slip, and impact on abrasion wear.

Wear duration curves show that the balls penetrate slower into 'wet' (high density) mixes, and mixes with high cement contents, and rapidly into 'dry' (low density) mixes and mixes with low cement contents.

The bearing pressure beneath the balls decreases as the balls penetrate further into the surface, resulting in curves which approximate a quadratic function with exponential $n=0,5$.

An attempt was made to find an alternative abrasion index. One alternative was to use the slope, n , of the MA20 formula expressed in logarithmic form. Similarly an n value based on the slope of the 'volume of the abraded groove versus 'revolutions' graph was considered. Although the high correlation coefficients were obtained for the revolutions increasing from 1000 to 5000 on an individual mix, indicating a constant rate of volume loss, the data did not correlate as well with compressive strength results as the standard I_a used in MA20, $I_{a_{MA20}}$, or $I_{a_{INT}}$.

Therefore in the absence of a better means of expressing abrasion resistance, it is recommended that either of these two indices be retained. Alternatively direct measurement of depth at 5000 revolutions, P_{5000} , or direct measurement/calculation of volume, V_{5000} may also prove useful.

The differences between the Australian MA20 and MA20SA are set out, other than limiting criteria, as these are discussed in chapter 15 and 16.

The relatively high variability of these tests has been addressed in terms of further modifications to the apparatus and test method, resulting in the CMA20 specification (see appendix A.6), but to date this apparatus has yet to be built.

Finally, the strengths and weaknesses of MA20 are considered.

For a comprehensive comparison between the MA20, wirebrush, and ASTM C418 abrasion tests, and a recommendation on which of the three tests is best suited for the industry, reference should be made to chapter 12.

An unsatisfactory ending

The story of the MA20 (and MA20SA) test has an unsatisfactory ending. It may be personified as a young promising film star who rapidly rose to fame, and then faded away after a few years, never to rise again. The test made its debut in Perth, Australia, in 1983, and by 1986 [Rourke(1986)] was widely acclaimed. However, it soon became evident that the test had some serious flaws, (1) a high variability, and (2) it did not seem to be able to ensure that factory made blocks that passed the test's (interim) criteria would necessarily be wear-resistant once installed and trafficked. A major attempt at rehabilitation was made in 1992[Shackel(1992)]. But already the tide had turned and an old rival in the form of the SSC test came to the fore. In 1993[Shackel(1993b)] and 1994[Shackel(1994)] the two rivals were competing in the same limelight, under the careful eye of a the critics (the Australian paving industry), but by 1996[Humpula(1996)] the curtain was coming down for MA20. By 1997 the show was over, as the SSC, with some minor modifications and re-baptized as AS/NZS 4456.9, was adopted as the official abrasion test by the combined Australian and New Zealand Standards organizations.

MA20SA's fortunes were in many ways always tied to those of MA20. The test, first used in South Africa in 1987 by the writer, was on the point of being adopted by the CMA in 1993, in a modified improved form, CMA20 (i.e. incorporating all the refinements of Shackel(1992)'s study). However, it was stillborn, given the misgivings in Australia at that time.

Interestingly, the ASTM C779 Proc C test, the father of MA20 lives on in the USA, and is also being used in other countries (Thailand, Japan). The roots of the ASTM test seem to go back as far as the 1930/40s, in the form of the Davis ball rest, reported on by Smith(1958). It seems to have been modified at least twice Prior(1966), and finally emerged as ASTM C779 Proc C. It further appears that the rise and fall of its Australian offspring never caused the USA test to loose any popularity. On the contrary it seems to have an ever increasing following, being preferred by some to other ASTM abrasion tests. Ghafoori – see table 9.5 - has consistently preferred it to the ASTM C418 or ASTM C944 tests).

Ghafoori(1992) stated that the 'use of ASTM C779, Proc C, ball bearing test was 'very successful' in evaluating the relative performance of various block surfaces, and that it is 'the most appropriate testing method to simulate traffic wear'.)

Table 9.5 lists, chronologically, some of the authors who used 'rolling steel balls' in their investigations. The different names of the tests are indicated. The rise and steady growth of the ASTM C779 Proc C may be discerned, as may the rise and fall of MA20 and MA20SA.

In a thorough analysis of MA20, Shackel(1992) concluded that 'providing an adequate amount of data is obtained, the MA20 abrasion test can provide a simple and rapid indicator of the abrasion resistance of pavers.' Given this statement and the many advantages of this test, catalogued in this chapter, and given the ongoing and increasing use of ASTM C779 Proc C, the writer believes that the demise of MA20 is an unsatisfactory ending.

Table 9-5 Various forms of Rolling Steel Ball Abrasion Tests and Investigating Authors

Year of Paper	Author	Abbreviated name	Country of Testing
1957	Sawyer	DIN 51951 (1953)	Germany
1958	Smith	Davis test	USA
1966	Prior	ASTM C779 Proc C	USA
1986	Rourke	MA20	Australia
1988	Papenfus	MA20SA	South Africa
1990	Fernandez	ASTM C779 Proc C	Canada
1991	Holland	MA20SA	South Africa
1991	Robertson	MA20SA	South Africa
1991	Laplante	ASTM C779 Proc C	Canada
1992	Shackel	MA20	Australia
1992	Ghafoori	ASTM C779 Proc C	USA
1993	Sukandar	ASTM C779 Proc C	USA
1994	Rocha	MA20SA	South Africa
1996	Humpula	MA20	Australia
1997	Tangtermsirikul	ASTM C779 derivative	Thailand
1997	Ghafoori	ASTM C779 Proc C	USA
1998	Harashima	ASTM C779 Proc C	Japan
1999	Ghafoori	ASTM C779 Proc C	USA
2000	Malhotra	ASTM C779 Proc C	USA

Recommendation

Rocha(1994) commented on the usefulness of MA20, but observed that its repeatability needed to be addressed, and recommended changes according to Papenfus(1994)'s recommendations (i.e. those incorporated in CMA20).

The writer recommends that a further series of parallel abrasion tests be done on the sides of control concrete cubes, to determine the difference in variability of MA20, MA20SA, CMA20 and ASTM C779 Proc C. Should the outcome show that CMA20 or ASTM C779 adequately address the inherently high variability of MA20, then they should be seriously considered as an abrasion test for the paving industry in South Africa.